Master in Chemical Engineering

Hydrocarbons Thermal Cracking Selectivity Depending on Their Structure and Cracking Parameters

Thesis of the Master's Degree

Development Project in Foreign Environment

FEUP
Universidade do Porto
Faculdade de Engenharia

INSTITUTE OF CHEMICAL TECHNOLOGY PRAGUE

Cláudia Sofia Martins Angeira

Erasmus coordinator: Eng. Miguel Madeira

Examiner in FEUP: Eng. Fernando Martins

Supervisor in ICT: Doc. Ing Petr Zámostný

July 2008

Acknowledgements

I would like to thank Doc. Ing. Petr Zámostný for the opportunity to hold a master's thesis in this project, the orientation, the support given during the laboratory work and suggestions for improvement through the work.

Abstract

This research deals with the study of hydrocarbon thermal cracking with the aim of producing ethylene, one of the most important raw materials in Chemical Industry. The main objective was the study of cracking reactions of hydrocarbons by means of measuring the selectivity of hydrocarbons primary cracking and evaluating the relationship between the structure and the behavior. This project constitutes one part of a bigger project involving the study of more than 30 hydrocarbons with broad structure variability. The work made in this particular project was focused on the study of the double bond position effect in linear unsaturated hydrocarbons.

Laboratory experiments were carried out in the Laboratory of Gas and Pyrolysis Chromatography at the Department of Organic Technology, Institute of Chemical Technology, Prague, using for all experiments the same apparatus, Pyrolysis Gas Chromatograph, to increase the reliability and feasibility of results obtained. Linear octenes with different double bond position in hydrocarbon chain were used as model compounds.

In order to achieve these goals, the primary cracking reactions were studied by the method of primary selectivities. The yields of primary products were obtained at low conversion (bellow 30 %) and then the primary selectivity was obtained by extrapolation to conversion limiting to zero. The formation of products observed by experiments can be explained mainly by radical reactions and the main reactions occurred are β-scission of C-C bond, hydrogen abstraction and radical intramolecular isomerization. It was found that the reactions of alkenyl radicals of an allyl character are the most important factor in determining the abundance of different products and the delocalized nature of such radicals plays a substantial role.

In the computation part of the project, the possibility of estimating main product yields obtained at high conversion from primary selectivities by an artificial neural network, was evaluated. Despite the very limited data set, it was possible to obtain reasonably good generalization using feed-forward neural network.

Keywords: linear unsaturated hydrocarbon pyrolysis, ethylene production, primary cracking selectivity, ANN modeling.

Contents

1 Introduction

Production of lower olefins, like ethylene and propylene, it is a fundamental process in chemical industry for the reason that the worldwide demand for these compounds is higher than any other chemicals. They are the primary feedstock in the production of polymers, man-made fibers and most plastics [1].

Ethylene, the lightest olefinic hydrocarbon, does not occur freely in nature. It represents the largest-volume petrochemical produced in the world and has not direct end uses, being used almost exclusively as a chemical building block in the organic chemical industry. Propylene is a byproduct in ethylene production and it is mainly used to produce polypropylene [2].

Nowadays, most of ethylene is produced by the steam cracking process. In this process, suitable hydrocarbons are heated to very high temperatures, in presence of steam, to split ("crack") the molecules into low molecular alkenic products. Feedstock selection is a very important parameter – along with the capacity, pyrolysis furnace operation conditions, reactor design and strict standardization of conditions – to achieve the optimum yield of desired products. The hydrocarbon feedstocks used in ethylene pyrolysis are shown in Figure 1 and, as we can see, naphta is the most common feedstock (45%).

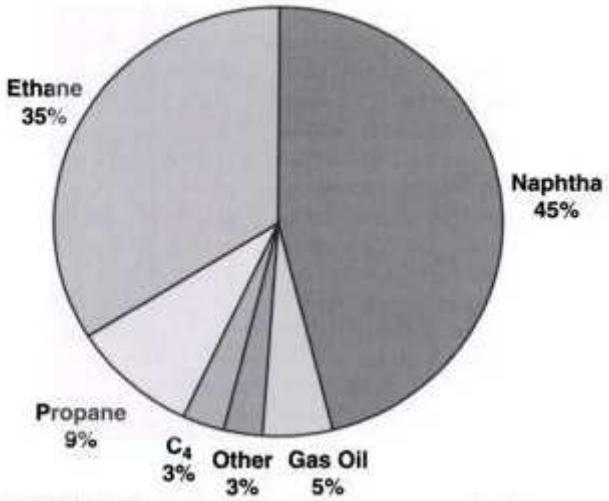

Figure 1: Worldwide feed slate (percentage of ethylene production capacity) [3]

However, the rapid development of petrochemical industry led to the lack of suitable raw materials for pyrolysis process and became necessary to search for other feedstocks, such as medium and heavy oils - kerosene, gas oil and vacuum distillate. Pyrolysis of these substances is

difficult because it leads to increase coke formation and ethylene production decreases. On the other hand, this development provides the utilization of other feedstocks like hydrocarbon streams in the refineries and petrochemical companies that have little meaning and need to be recycled.

Experimental papers presented in literature are mostly aimed at studying saturated hydrocarbons and other selected hydrocarbons. Therefore, it is important to study the behavior of unsaturated hydrocarbons.

There are two main questions to be resolved by the laboratory experiments. Low-temperature data disclose the primary cracking mechanisms and thus, allow further mechanistic models of industrial pyrolysis reactors developments, especially to improve the prediction of pyrolysis products. Laboratory results of high-temperature experiments are beneficial to developing methods of transmission of laboratory data to the operational scale.

Evaluation of raw materials in view of thermal cracking product distribution often takes advantage of mathematical modeling. The empirical models are more closely aimed at the evaluation of cracking products yields depending on the feedstocks composition. The advantage of empirical models lies simply in the characterization of pyrolyzed feedstocks and the high reliability of predicted yields [4]. Therefore, such an empirical model – artificial neural network (ANN) – was chosen to predict the cracking product yields.

2 State of Art

The thermal decomposition of alkanes has been extensively studied since the early thirties. This led to the discovery of the reactive intermediates: the carbon free radicals and the chain reactions in organic chemistry. In the late 1940s and early 1950s kinetic – mechanistic models of a multitude of carbon free radicals and the chain reactions have been recognized. Recognized as the standard modes of hydrocarbon decompositions, helping the description of the key pyrolysis parameters and their interrelationships and consequently, allowing greater understanding of cracking furnace design and yield prediction [3, 5, 6]. The key principles in hydrocarbon pyrolysis that can be drawn from thermodynamics and kinetics are:

- Low residence time – This is the fundamental key to greater cracking selectivity, because it can be linked to the fact that ethylene is produced primarily by first-order dissociation of larger molecules. Hence, to minimize residence time without exceeding heat flux limits, the optimal cracking coil should have a small diameter with an adequate length. The coil length-to-inside diameter ratio is an important design parameter, being the optimal value approximately 500;

- Low hydrocarbon partial pressure – Since the thermal cracking reaction results in molecular expansion, system pressure should be at minimum (Le Châtelier principle);

- High cracking conversion – Maximum ethylene yield corresponds to high conversion operation. Ethylene production pyrolysis is a high heat intensity process and the heat of cracking depends on feedstock and conversion. Consequently, conversion is a function of both residence time and temperature.

Collaterally, depending on the feed, pyrolysis also produces valuable byproducts, such as propylene, butadiene, benzene, gasoline and hydrogen. The less valuables coproducts include methane and fuel oil. An important parameter in the design of commercial cracking coil is the optimal selectivity to produce the desired product slate for maximizing economic returns. The product distribution is affected by feed specifications, reactor coil, residence time, severity of operation and hydrocarbon partial pressure, as was referred to above.

2.1 Mechanisms of Hydrocarbon Pyrolysis

Available information on the mechanism of pyrolysis reactions are often very inconsistent and incomplete, moreover, it mostly derived from individual laboratory pyrolysis of hydrocarbons.

Pyrolysis reactions of hydrocarbons can be divided in two groups – the primary and the secondary. Primary reactions comprise those leading to the first generation of pyrolysis products while the secondary include reactions involving the first generation products as educts. The hydrogen abstraction, β-scission of a C-C bond, and intramolecular isomerization are the typical examples of primary reactions. The product distribution of the primary reactions – the primary selectivity – can be used for studying the pyrolysis reactions mechanisms and with regard to the expected conversion for the industrial feedstock assessment as well [7].

It is also known that the pyrolytic reactions are very fast and strongly endothermic which require a great amount of heat delivered within the short residence time. Hydrocarbon pyrolysis reactions run mainly by radical mechanism, however, molecular reactions have also significant importance [8, 9]. In the first phase, pyrolysis is composed mainly of intermediate influenced kinetic reactions and in the final stage pyrolysis, on the opposite, it is controlled by the thermodynamic aspect of the process and, consequently, substances less stable, improve gradually their thermodynamic stability [10].

2.1.1 Radical Mechanism Reactions

The basic radical chain mechanism for the decomposition of hydrocarbons by thermal cracking was proposed, in pioneering works, by Rice [11] and Rice and Herzfeld [12]. Radical mechanism pyrolysis of hydrocarbons can be subdivided into three phases:

- Initiation
- Propagation
- Termination

The characteristic features of pyrolysis radical reactions are a long chain of repeated reactions regenerating radicals in the propagation stage of pyrolysis. The effect of termination and

initiation reactions, on the product yields, is therefore very small but they can still significantly affect reached conversion.

2.1.1.1. Initiation

The initiation phase takes place by the homolytic scission of a C-C bond, normally the weakest link (290 to 380 kJ.mol^{-1} [13]), in the substrate molecule producing two alkyl radicals. For example, in a molecule of octane:

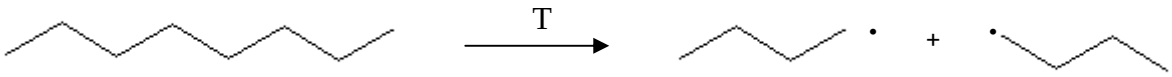

The C-H bond is relatively stable, with higher bond energy dissociation (340 to 440 kJ.mol^{-1}) [10, 13, 14]. For this reason these kind of bonds split significantly only when electron effects are attenuated or in unsaturated aromatic bonds (dissociation energy around 340 to 380 kJ mol^{-1}) [13, 14].

2.1.1.2. Propagation

Chain propagation involves many different reactions, including hydrogen abstraction, addition, radical decomposition and radical isomerization.

The number of possible radicals and reactions, in the propagation phase, increases rapidly as the chain length increases. The free-radical mechanism is generally accepted to explain hydrocarbon pyrolysis at low conversion [15].

Hydrogen transfer reaction is based on the abstraction of one hydrogen atom for formation of new radical a new molecule. Hydrogen abstraction is also dependent on C-H bond energies. As shown in Table 1, the declining strength of hydrogen bonds from primary to tertiary hydrogen leads to greater probability of secondary and tertiary radicals than primary radical:

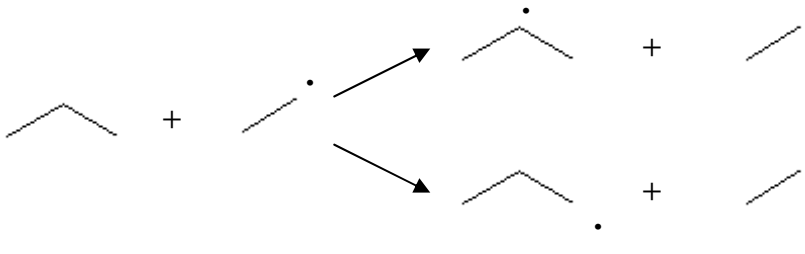

(main reaction)

(side reaction)

Table 1: C-H bond dissociation energy in saturated hydrocarbons

Link Type	**B.D.E. (kJ mol^{-1})** [16]
H – CH_3	440.0 ± 0.8
H – CH_2CH_3	411.1 ± 4.2
H – $CH(CH_3)_2$	398.2 ± 4.2
H – $C(CH_3)_3$	390.2 ± 8.4

On unsaturated hydrocarbons, the C-H bond in α-position to the unsaturated bond has the highest energy, whereas, the C-H bond in β-position has the lowest energy because of the conjugated effect with the multiple bonds. To comprise the differences in link energies is shown in Table 2, for example, all C-H bond dissociation energies on trans-4-octene.

Table 2: C-H bond dissociation energy in trans-4-octene

Link Type	**B.D.E. (kJ mol^{-1})** [14]
H – $CH_2(CH_2)_2HC{=}CH(CH_2)_2CH_3$	419.2
CH_3C **–** $\mathbf{H_2}CH_2HC{=}CH(CH_2)_2CH_3$	410.0
CH_3CH_2C **–** $\mathbf{H_2}HC{=}CH(CH_2)_2CH_3$	348.8
$CH_3(CH_2)_2$**H –** $C{=}CH(CH_2)_2CH_3$	429.9

An important group of reactions in the ongoing propagation phase of steam cracking process is radical isomerization. Radical isomerization may occur by shifting atoms or groups of atoms to another location. However, the most common in radicals with long chain is the primary isomerization, based on the internal hydrogen transfer from 1-4, 1-5 and 1-6 position through a

ring formation. These reactions include a transit state of five, six or even more (four, five or more carbon atoms and one hydrogen atom) [7, 17]. The most frequent isomerization is 1-5 position, for example:

- saturated compounds

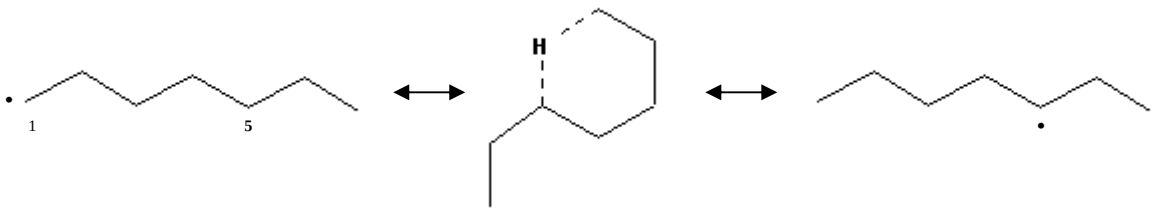

- unsaturated compounds

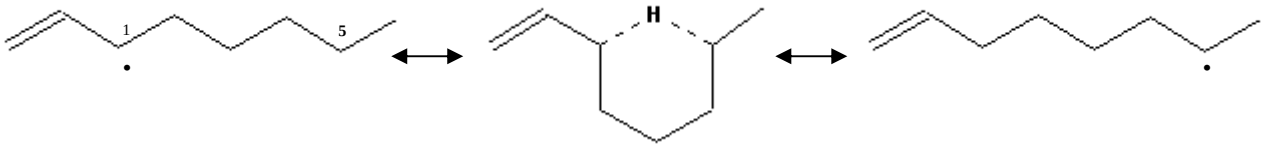

Another type of reaction in propagation phase is splitting. Since the activation energy for homolytic scission reactions is higher than activation energy for isomerization, the importance of isomerization is very low at high temperatures.

The most common splitting reaction is β-scission of C-C bonds. β-scission of C-H bond could happen too, but with less frequency because C-H bonds have higher bond dissociation energies than C-C bonds. This radical cleavage leads to the formation of olefins (a stable molecule, which is one of the products) and another radical, by shifting the electron to the carbon in the β-position:

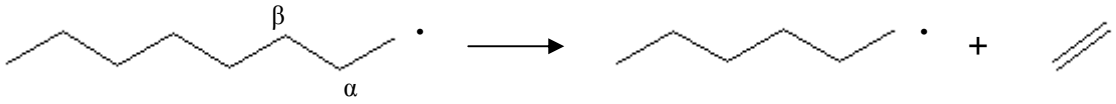

If the radical has a ramification in the α-position carbon to unmatched electron, the β-scission will generate in parallel different types of products, such as:

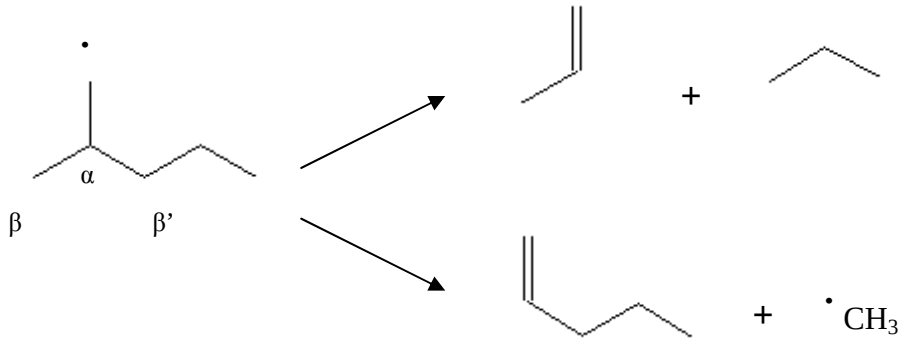

In case of a radical containing a multiple link in β-position to an unmatched electron it will cause the weakening of C-H bonds and the C-C bond scission will have a similar rate as C-H bond scission, for example:

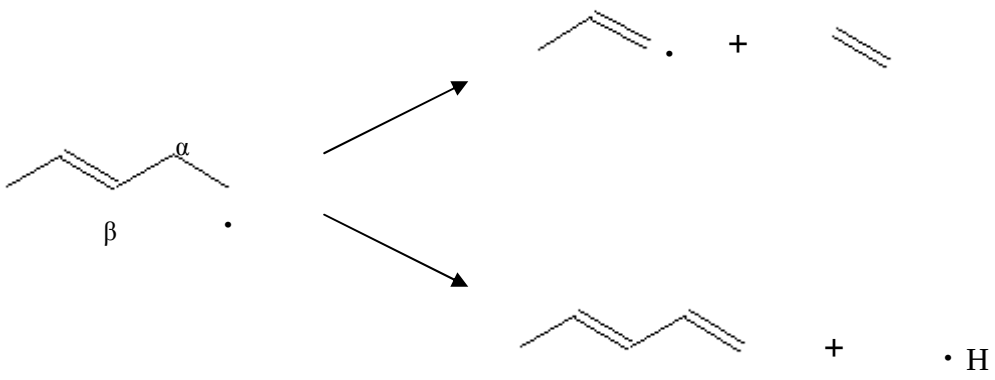

2.1.1.3. Termination

The last phase of free-radical reactions, termination, is the opposite to initiation, causing the disappearance of radicals (forming stable products). In termination, could happened addition between two radicals and also reactions between radicals and the reactor wall.

The most frequent termination reaction is a merger of two radicals in one molecule, such as:

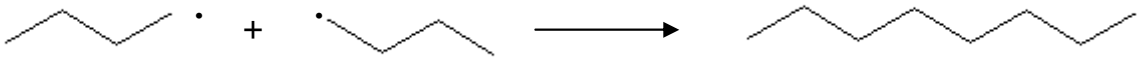

The chain termination could also occur with collision of radicals on the reactor wall, in which radicals disappeared. The main problem in scaling-up laboratory data to industrial condition is normally the wall effect. Radical are extinguished an order of magnitude faster on metal surfaces than on non-metallic (laboratory quartz reactors), because of the high thermal conductivity and redox properties of metal materials. On the other hand, if laboratory reactors are metallic, the wall effect is stronger than in their industrial counterparts because of a relatively large reactor-wall surface area and a small reaction volume [18].

2.1.2 Molecular Reactions

When a high conversion of feedstock is promoted by radical chain reaction, molecular reactions of individual products of pyrolysis radical reactions could happen. Typical molecular reactions are dehydrogenation, isomerization and cyclo-addition known as Diels-Alder reaction. The following reactions are typical examples of the first two types of molecular reactions [9]:

$$CH_3CH_3 \longrightarrow CH_2 = CH_2 + H_2 \quad \text{(dehydrogenation)}$$

$$CH_3CH_2CH{=}CHCH_2CH_3 \longrightarrow CH_3CH{=}CHCH_2CH_2CH_3 \quad \text{(isomerization)}$$

The main mechanism for aromatic products formation by pyrolysis is through Diels-Alder (reaction between a conjugation diene and a substituted alkene, commonly termed the dienophile, to form a substituted cyclohexene system) and subsequent dehydrogenation, such as [19]:

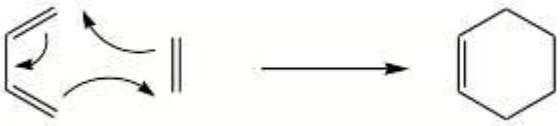

2.2 Pyrolysis of Unsaturated Hydrocarbons

The studies involving unsaturated hydrocarbon are too limited. Some years ago it was not important to know the intervention of the unsaturated hydrocarbons in pyrolytic process because it was common to use typical feedstocks in ethylene production and there was no need to know the influence of each compound in the process. However, the typical feedstocks have been changed because petroleum fraction has become a very expensive raw material to ethylene production and new feedstocks are forming by waste treatment processes. To be sure if ethylene production will be efficient it is necessary to make some preliminary estimation. For this it is very important to know the relationship between the products and the feedstocks.

The thermal decomposition of olefins usually results in the formation of predominance of a diolefin and a paraffinic hydrocarbon or in the formation of two other olefins. The particular materials which predominate when olefins are cracked depend largely upon the configuration of the olefin which is cracked. What is meant by configuration is the position of the double bond and the position of the side chains, if any [20].

In this work, what will be studied is the difference between the double bond position in olefins in the steam cracking process and the results obtained will be used to train an artificial neural network to predict cracking product yields at high temperatures. Unsaturated structures will be compared according to their tendency to undergo radical additions.

2.3 Predictions of Thermal Cracking Yields

In recent years, a considerable effort has been devoted to the development of computer programs for the simulation of the thermal cracking of pure hydrocarbon and their mixtures. Mathematical modeling is the most attractive solution because it has the advantage that once the model is developed, results can be gathered easily and computer simulations take only a limited time [21-24]. One of the major challenges in this approach consists in developing a fundamental reaction network. Moreover, fundamental kinetic models require a detailed feedstock composition and obtain this information for complex hydrocarbon mixtures are not straightforward.

Simulation models based upon radical reactions occurring in the reaction mixture have the potential to predict product distribution as a function of feed properties and operation conditions. This type of information generated from mechanistic modeling has also great practical value for the design of reactors, optimization of technologies and into scale-up laboratory results.

To predict the cracking product yields the empirical model selected is artificial neural network (ANN).

2.3.1 Artificial Neural Networks - History

Artificial neural networks are, as their name indicates, computational networks which attempt to simulate, in a gross manner, the networks of nerve cell of the biological central nervous system [25].This simulation is a gross cell-by-cell simulation and it borrows from the neurophysiological knowledge of biological neurons and of networks of such biological neurons. Its development began approximately 50 years ago, motivated by a desire to try both to understand the brain and to emulate some of its strengths.

Artificial neural networks emerged after the introduction of simplified neurons by McCulloch and Pitts in 1943. These neurons were presented as models of biological neurons (Figure 2) and as conceptual components for circuits that could perform computational tasks. The basic model of the neuron is founded upon the functionality of a biological neuron [26].

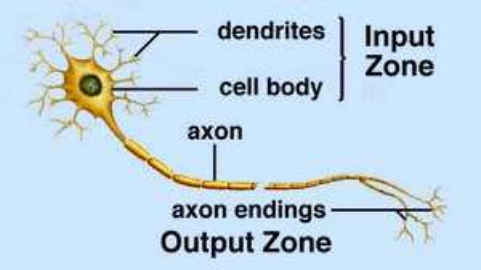

Figure 2: Scheme of a biological neuron

However, the field of neural networks looks at a variety of models with a structure roughly analogous to that of the set of neurons in the human brain. Artificial neural networks can be most adequately characterized as "computational models" with particular properties such as the ability to adapt or learn, to generalize, or to cluster and organize data.

To capture the essence of biological neural systems, an artificial neuron is defined as follows:

- It receives a number of inputs (either from original data, or from the output of other neurons in the neural network). Each input comes via a connection that has a strength (or *weight*); these weights correspond to synaptic efficacy in a biological neuron. Each neuron also has a single threshold value. The weighted sum of the inputs is formed, and the threshold subtracted, to compose the *activation* of the neuron (also known as the post-synaptic potential of the neuron);

- The activation signal is passed through an activation function (also known as a transfer function) to produce the output of the neuron.

To characterize a neural network it is necessary to define:

  - *architecture* – its pattern of connection between the neurons;

  - *training or learning algorithm* – its method of determining the weights on the connection;

- *activation function* – neuron's internal state, which is a function of the inputs it has received.

2.3.2 Neuron Model

The simplest neural network is a neuron with a single scalar input and with a single layer, as shown in Figure 3.

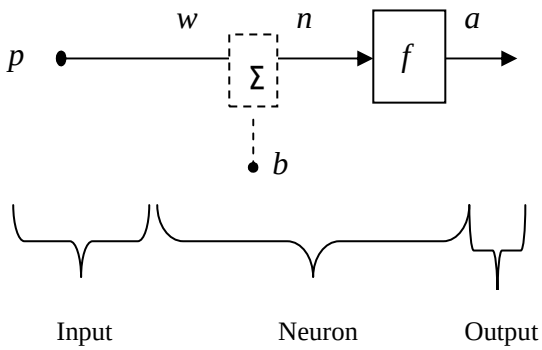

Figure 3: Scheme of the simplest neural network

The scalar input *p* is transmitted through a connection that multiplies its strength by the scalar weight *w*, to form the product *wp*, again a scalar. In this basic network, represented above (without considering the dotted part), the scalar output *a* is produced by the transfer function *f* with the weight input *wp* as the only argument. If the network has a bias *b* (consider the dotted part in Figure 3), the only difference is that the new argument of the transfer function is *n*, the sum of the weighted input *wp* with the bias *b* [27].

A network can have several layers and all of them play different roles. The layer which produces the network output is called output layer and the others are called hidden layers.

For instance, a network with two layers, where the first layer is sigmoid and the second is linear, can be trained to approximate any function arbitrarily well. This kind of network is frequently used in backpropagation algorithms [26].

2.3.3 Backpropagation Algorithm

Backpropagation was created by generalizing the Widrow-Hoff learning rule to multiple-layer networks and non-linear differentiable transfer function. The backpropagation algorithm has a supervised training. This means that for a sequence of training input vectors there may exists

target output values. The training continues until the network is able to provide the expected response [27].

The three transfer functions most commonly used in backpropagation are log-sigmoid, tan-sigmoid and linear. Normally, linear transfer function is used in the output layer in order for the outputs to take on any value [28].

There are several different training algorithms, but all of them use the gradient of the performance function to determine how to adjust the weights to minimize performance. The training function chosen, in this project was Levenberg-Marquardt and the performance function was the mean sum of square of network errors. Levenberg-Marquardt function was designed to approach second-order training speed using Jacobian matrix instead of Heassian matrix, like quasi-Newton methods.

One of the troubles that usually occur during neural network training is over-fitting. It happens when the error on training set is driven to a very small value, but when new data is presented to the network the error is large. The network has not learned how to generalize to new situations, it only memorized training examples.

There are two ways to improve generalization: regularization and early stopping.

Regularization consists in modifying the performance function and can be done manually, but is difficult to determine the optimum value for the performance ratio value. It is usually made by Bayesian regularization (automated regularization) because is the easiest method to achieve optimal regularization.

In early stopping, data will be divided in training set and in validation set. The first is used for computing the gradient and updating the network weights and biases. The error on the validation set is monitored during the training process. The validation error will normally decrease during the initial phase of training, as the training set error. However, when the network begins to overfit the data, the error on the validation set will typically begin to rise. When the validation error increases for a specific number of iterations, the training is stopped, and the weights and biases at the minimum of the validation error are returned [27].

3 Technical Description

The experimental part of the project is based on intensive application of instrumentation of micro-pyrolysis technique with pulse sample injection and multi-column and mass-spectrometric analysis, installed in the Laboratory of Gas and Pyrolysis Chromatography[1]. This technique was developed and extensively used for investigating the research projects of the National Center for Crude Oil Processing and it already provided its reliability.

In laboratory experiments, four commercial hydrocarbons were used. The purity tests were made using gas chromatograph equipped with mass spectrometric detector (GC-MS) to identify the nature of impurities and their amount was determined by employing GC-FID. Pyrolysis reactions run in pyrolysis gas chromatograph system under different conditions for each feedstock.

3.1 Feedstock

The feedstock studied is composed by alkenes, unsaturated hydrocarbons, with different double bond position, such as, 1-octene, trans-2-octene, trans-3-octene and trans-4-ocetene.

Features of raw-materials are shown in Table 3. Purity of hydrocarbons was measured by pyrolysis gas chromatography with the furnace heating turned off (to prevent pyrolytic reactions) and impurities were determined in mass spectrometer.

Table 3: Feedstock characterization

Sample	Producer	Purity (%)
1-octene	Fluka	99.459
trans-2-octene	Aldrich	98.209
trans-3-octene	Fluka	98.996
trans-4-octene	Aldrich	99.467

[1] The work on the Project was carried out in the Laboratory of Gas and Pyrolysis Chromatography at the Department of Organic Technology, Institute of Chemical Technology, Prague

3.2 Pyrolysis Gas Chromatography

Pyrolysis gas chromatography is based on the direct connection between pulse micro-reactor and the set of gas chromatographs (Figure 4). The pyrolysis reactions proceed in the furnace where the micro-reactor is located.

Figure 4: Pyrolysis gas chromatograph Shimadzu

The products of cracking are separated by a set of four analytical columns switched during the analysis by a set of switching valves. The analysis of cracking products is based on separated analysis of pyrolysis gas, pyrolysis gasoline and pyrolysis oil [6].

3.2.1 Equipment Description

The apparatus (Figure 4) used in laboratory study of hydrocarbon pyrolysis was compiled from a standard pyrolysis unit Pyr-4A Shimadzu and on-line dual gas chromatography unit (2 x GC 17A Shimadzu). The pyrolysis micro-reactor, placed in the pyrolyser is made of a quartz tube and it is a standard component of the pyrolysis unit Pyr-4A Shimadzu. The length of the reactor is 180 mm, its inner diameter is 3 mm and it is filled by carbide silica pellets to induce higher turbulent flow of the reaction mixture with an average residence time in the hot zone about 0.2 s. The

feedstock and steam is sent to the reactor to be heated in an electric furnace, achieving the desired temperature (up to 820 ºC) by means of radiation [6]. The axial temperature profile in the reactor is shown in the Figure 5, and it is characterized by a relatively short reaction zone, as well as by soaring and plunging temperatures in the heating and cooling zones, respectively.

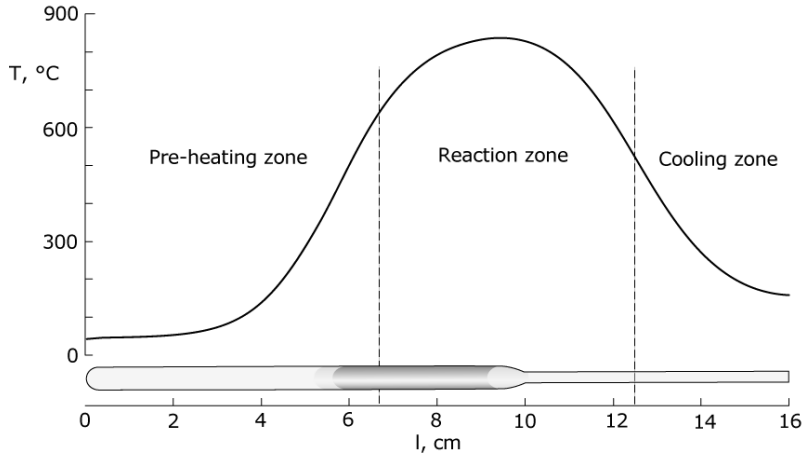

Figure 5: Typical temperature profile for a reaction mixture in the laboratory pyrolysis reactor [6]

The gas chromatographic analysis of the reaction mixture is carried out in four capillary columns placed in a dual on-line chromatograph with four detectors and three switching valves (Figure 6).

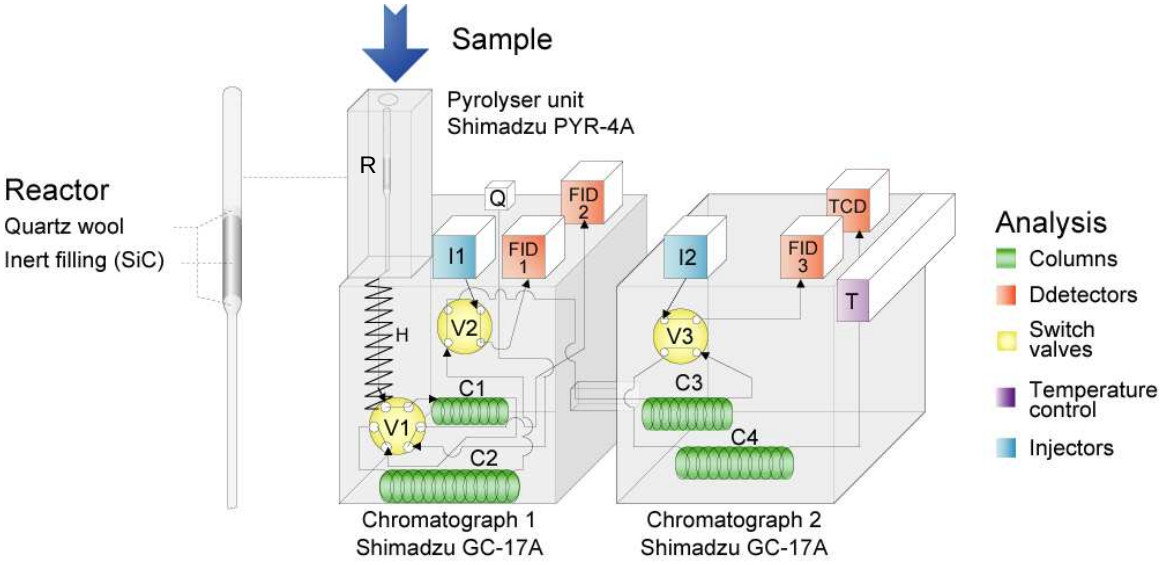

Figure 6: Pyrolysis reactor scheme. R: reactor; C_1-C_4: capillary columns; V_1-V_3: change-over valves; I_1-I_2: injection ports; FID_1-FID_3: flame ionization detectors; TCD: thermal conductivity detector; Q: auxiliary carrier gas source, H: heater

The combination of two chromatograph units is necessary to achieve different temperature programs in the different branches of the analytical path. The first chromatograph is equipped

with two flame-ionization detectors FID_1 and FID_2, an injector I_1 and an auxiliary carrier-gas source Q. The chromatograph oven accommodates two capillary columns (K_1 and K_2) and two switching valves (V_1 and V_2). The temperature of the capillary line connecting the reactor with valve V_1 is maintained with a separate thermostat H controlled independently from the column oven. The second chromatograph includes a flame ionization detector FID_3, a thermal conductivity detector TCD and an injector I_2. The column oven contained capillary columns, K_3 and K_4, and a switching valve V_3. The connection between the two chromatographs is also heated. The main function of injectors I_1 and I_2 is to control the carrier-gas flow rate; sample introduction through them is practiced only during equipment testing. Hydrogen and air are supplied to all the flame-ionization detectors and the carrier gas used is nitrogen.

The inlet of the reaction products into the V_1 valve is made by a short deactivated column, heated to 250 °C, regardless the GC temperature program to ensure quick and uniform transfer of the sample into the chromatographic column C_1. The deactivation and high temperature of this line, in contrast to the initial programming of the column temperature, are designed to suppress the separation of the condensation of the mixture into individual components and to prevent the condensation of the pyrolysis products. Valves V_1-V_3 are sequentially switched in four periods of time to analyze pyrolysis products in fractions.

The chromatographic analysis traces all groups of pyrolysis products - pyrolysis gases, pyrolysis naphtha, and pyrolysis oils (Annex A). The evaluation of pyrolysis product yields is based on the sequential analysis:

- in the first place, the C_{13} hydrocarbons (and higher) are retarded in the C_1 column, other liquid and gaseous pyrolysis products continue to the next columns;
- hydrocarbons from the C_1 column are analyzed on the FID_2 detector after the V1 valve switchover;
- hydrogen and methane from the C_4 column are analyzed on the TCD detector, and hydrocarbons C_7-C_{12} from the C_2 column are analyzed on the FID_1 detector after the V_2 valve switchover.
- finally, hydrocarbons C_2-C_6 from the C_3 column are analyzed on the FID_3 detector after the V_3 valve switchover.

Alternatively, the TCD detector can be removed from the analytical path and the detection of all gaseous products (excluding hydrogen) can be performed using the FID_3 detector. This modification can improve the analysis reproducibility and cut down the analysis time at the cost of missing hydrogen concentration, since the hydrogen cannot be detected on FI detectors. This tradeoff can be advantageous in studies, where series of similar feedstocks are compared, because in such cases the yields of hydrogen are relatively small (approx. 2 wt. %), steady throughout the whole series and usually not the point of interest.

3.2.2 Laboratory Procedure

Laboratorial experiments consist in injecting 0.3 μL of sample, into the nitrogen stream in the pyrolysis reactor through the septum, by means of a special syringe with a long needle. Samples had to be injected to the immediate vicinity of the inert filling upper boundary to prevent sticking sample to the reactor wall in the colder zone.

The total length of the analysis in this arrangement is 50 minutes. High conversion experiments were conducted at 810 °C. Discharge carrier gas was in all experiments 100 $ml.min^{-1}$ and pressure of 400 kPa. The standard conditions were chosen so for all feedstocks in the light pyrolysis materials will reach a similar conversion as usual for industrial pyrolysis [28]. Low conversion experiments were conducted at 620 °C at different residence times in reactor (variation in carrier gas flow between 50 and 400 $mL.min^{-1}$) to achieve feedstock conversion in the range of 5 to 30%. Optimal temperature, allowing to reach desired conversion, was determined experimentally. Each experiment was repeated at least two times to produce results with accuracy and reproducibility.

The reliability of measurement is established by regular analysis of a standard mixture of hydrocarbons, determining the response factors for each detector (Table 4). Standard pyrolysis peaks are measured at low temperature to avoid the mixture pyrolysis (Annex A).

Table 4: Detectors response factors at standard conditions of sensitivity

Detector	Response factor
FID_1	0.1075
FID_2	0.0149
FID_3	1.0000

3.2.3 Experimental Data Evaluation

Pyrolysis gas chromatograph is connected to a computer having software (Class VP) installed to control and evaluate the experiments with methods specially created to evaluate the chromatograms obtained. The responses of individual detectors can be monitored real-time during analyses in form of chromatograms displayed in the computer. That software enables the integration of each detector's digital signal. Acquired partial data will then be further processed in Excel.

The obtained amount of product can be expressed in several ways. In this work yields and selectivity are used. It expresses the ratio between mass fraction of product and achieved conversion of pyrolyzed feedstock:

$$y_i = \frac{w_i}{x} \cdot 100 \qquad (3.1)$$

where, y_i is the yield of product *i* (wt. %), w_i is the mass fraction of product *i* (wt. %) and *x* is the attained conversion of pyrolyzed compound (%).

The relationship between selectivity and yield is given by the following expression:

$$S_i = y_{i\cdot} \frac{M_i}{M_{feedstock}} \qquad (3.2)$$

in which S_i is the selectivity of product $_i$ (mol_i / $mol_{feedstock}$%), y_i is the yield of product *i* (wt. %) and *M* is the molecular weight.

3.3 Pyrolysis Gas Chromatography with Mass Spectroscopy

The apparatus consists in pyrolysis gas chromatograph (PYR 4A Shimadzu) with a mass spectrophotometer (QP 2010 Shimadzu) coupled, Figure 7. The device can be used for pyrolysis experiments or only for tradition gas chromatography with mass spectroscopy (if the temperature set in the device is too low that pyrolysis reactions don't occur). In this work, the last option was the only one used to know the impurities of the feedstock.

Figure 7: Pyrolysis Gas Chromatogram with Mass Spectrometer Shimadzu

3.4 Artificial Neural Network simulations

The experimental results obtained are not enough to train a network because only four compounds were studied. Also, the hydrocarbons studied are all linear unsaturated with 8 carbon atoms, and to achieve better results, experimental data from pyrolysis of saturated and branched hydrocarbons (measured for other project) was included in the training set.

The training of neural network was carried out using Levenberg-Marquardt optimization method in the MATLAB Neural Networks Toolbox.

4 Results and Discussion

The results obtained come essentially from laboratorial pyrolysis experiments and Neural Network simulations.

During the laboratorial experiments, four linear unsaturated hydrocarbons were studied. The hydrocarbons were pyrolyzed not only at high conversions (high temperature, 810 ºC), but also at lower temperature (620 ºC), in order to achieve lower conversion to subsequent discussion of the mechanism of primary cracking. Primary cracking reactions form primary products which are the educts from secondary products, being important those study. Each laboratory experiment was repeated at least twice, and the results presented below are the arithmetic means of the measurements.

In order to create an artificial neural network with the aim of predict the pyrolysis product yields, experimental data from saturated and branched hydrocarbons were added to experimental data obtained from linear unsaturated hydrocarbons to increase the range of different structural compounds. The neural network was trained in MATLAB using Levenberg-Marquardt algorithm.

4.1 Pyrolysis of unsaturated hydrocarbons

In order to study the mechanisms of primary cracking, low-temperature experiments were carried out. The reaction temperature chosen was the same for all the samples to have more reliable comparison of data obtained. For the suitable temperature estimation, experiments at different temperatures (700 ºC, 650 ºC, 630 ºC and 620 ºC) were performed with the intention to reach the conversion between 5 and 25 % which will permit discovering the primary cracking selectivity. The best temperature achieved was 620 ºC.

The tables presented below in this section only contain the significant values for the discussion of results.

Results interpretation

The interpretation of low conversion experiments consisted in proposing the overruling mechanisms of cracking that should explain the formation of all major products. The reaction

mechanisms were proposed on the basis of radical reactions theory and published information on bond dissociation energies in hydrocarbon molecules. Some simplifying assumptions were made prior to proposing the models to limit the number of possibilities to evaluate. It was assumed that even if feedstocks initiation reactions present a step necessary for starting up the radical reactions that step will not have a significant effect on products composition, because most of radicals arise in the propagation phase, in particular by hydrogen transfer. Therefore, the initiation step in primary cracking mechanism is neglected. The most common reactions in radical mechanism are hydrogen abstraction and β-scission of C-C bond (the scission of bond in β-position to unmatched electron to produce olefin and transfer the unmatched electron to the carbon atom in β-position). The reaction mechanism proposed is based in scission and in radical isomerization, particularly from 1-5 position in the hydrocarbon chain. Termination occurs basically by hydrogen transfer (absorption or abstraction) or by merging of two radicals. Termination reactions by combination of radicals with the reactor wall do not have significant influence on the composition of products. The effect of molecular reactions is unknown and must be considered as one of potential reaction pathways.

There were made pyrolysis experiments for each feedstock at 620 ºC with variations in the carrier gas flow between 50 and 400 $mL.min^{-1}$. The results obtained for trans-4-octene are presented in Table 5 as example:

Table 5: Yields of products resulting from the pyrolysis of trans-4-octene and conversion for different flow rates at 620 ºC

Flow ($mL.min^{-1}$)	50	100	200	300	400
x (%)	29.3	19.4	9.8	5.7	4.8
Products			y(wt.%)		
Methane	3.3	2.1	1.5	1.1	0.7
Ethylene	17.6	14.8	12.2	10.6	7.6
Propylene	2.4	1.7	1.4	1.1	0.9
1-Butene	1.3	0.8	0.8	0.7	0.6
1,3 Butadiene	6.4	4.8	4.0	3.3	2.3
C_5-C_6unidentified	32.9	28.4	23.7	21.3	16.4
Octenes	1.3	1.2	2.6	3.2	4.3
Octadienes	13.2	20.1	28.6	40.1	42.2
Nonenes	9.4	19.2	14.8	16.4	14,9

Observing the table above, it is possible to see that the conversion of raw material decreases when carrier gas flow increases. Also, it is shown that when conversion increases the yields of products with less carbon atoms than the starting material, C_7^-, increase and the opposite happens to yields of products with the same or more carbon atoms than the feedstock, C_8^+.

The yield and selectivity of primary cracking are obtained extrapolating to zero conversion the results achieved for several experiments at low conversions. For a better viewing, an example is exposed in the Figure 8, the dependence of ethylene selectivity on trans-4-octene conversion. The experimental data is adjusted with a linear trend line, except the results obtained for methane, ethylene and propylene in trans-2-octene pyrolysis because the values have exponential trend and consequently, were adjusted with an exponential trend line.

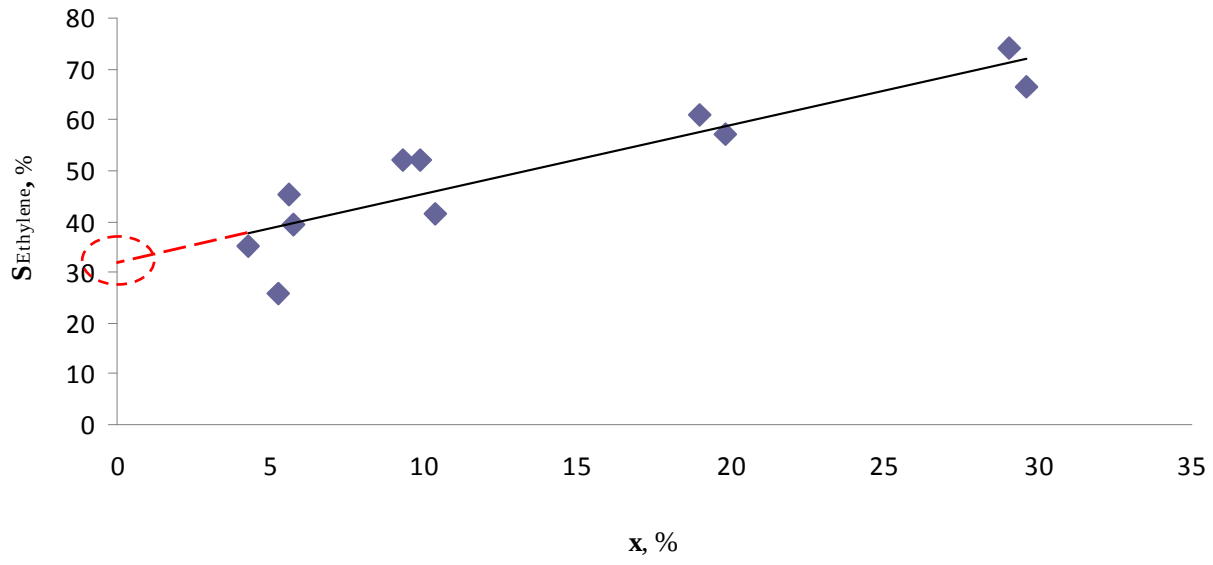

Figure 8: Primary selectivity of ethylene in trans-4-octene pyrolysis with a linear regression

This procedure was carried out for all samples and the values of yield and selectivity obtained for each product in each feedstock pyrolysis is presented in tables below:

Table 6: Yield and selectivity of products resulting from pyrolysis of 1-octene at 620 ºC

	y (wt. %)	**S** (mol/mol $_{feedstock}$ %)
Methane	0.1	0.6
Ethylene	2.2	8.9
Propylene	1.0	2.5
Butenes	0.6	1.2
1,3-Butadiene	0.7	1.4
C_5-C_6 unidentified	2.8	4.0
Octenes	44.0	44.0
Octadienes	28.1	28.6
Nonenes	23.9	21.3

Table 7: Yield and selectivity of products resulting from pyrolysis of trans-2-octene at 620 ºC

	y (wt. %)	**S** (mol/mol $_{feedstock}$ %)
Methane	0.2	1.6
Ethylene	3.2	12.6
Propylene	0.8	2.0
Butenes	2.0	4.0
1,3-Butadiene	1.4	2.9
C_5-C_6 unidentified	6.5	9.3
Octenes	42.4	42.4
Octadienes	38.9	39.6
Nonenes	21.8	19.4

Table 8: Yield and selectivity of products resulting from pyrolysis of trans-3-octene at 620 ºC

	y (wt. %)	**S** (mol/mol $_{feedstock}$ %)
Methane	0.2	1.2
Ethylene	2.3	9.2
Propylene	0.6	1.6
Butenes	0.3	0.6
1,3-Butadiene	1.0	2.0
C_5-C_6 unidentified	6.7	9.6
Octenes	19.8	19.8
Octadienes	48.1	49.0
Nonenes	34.0	30.2

Table 9: Yield and selectivity of products resulting from pyrolysis of trans-4-octene at 620 ºC:

	y (wt. %)	**S** (mol/mol $_{feedstock}$ %)
Methane	0.4	3.1
Ethylene	7.9	31.7
Propylene	0.7	1.9
Butenes	0.5	0.9
1,3-Butadiene	2.2	4.6
C_5-C_6 unidentified	16.8	24.1
Octenes	4.0	4.0
Octadienes	44.0	44.8
Nonenes	15.3	13.6

For a better viewing and comparison between the primary selectivities of products for all feedstocks these values are figured in the following column graph:

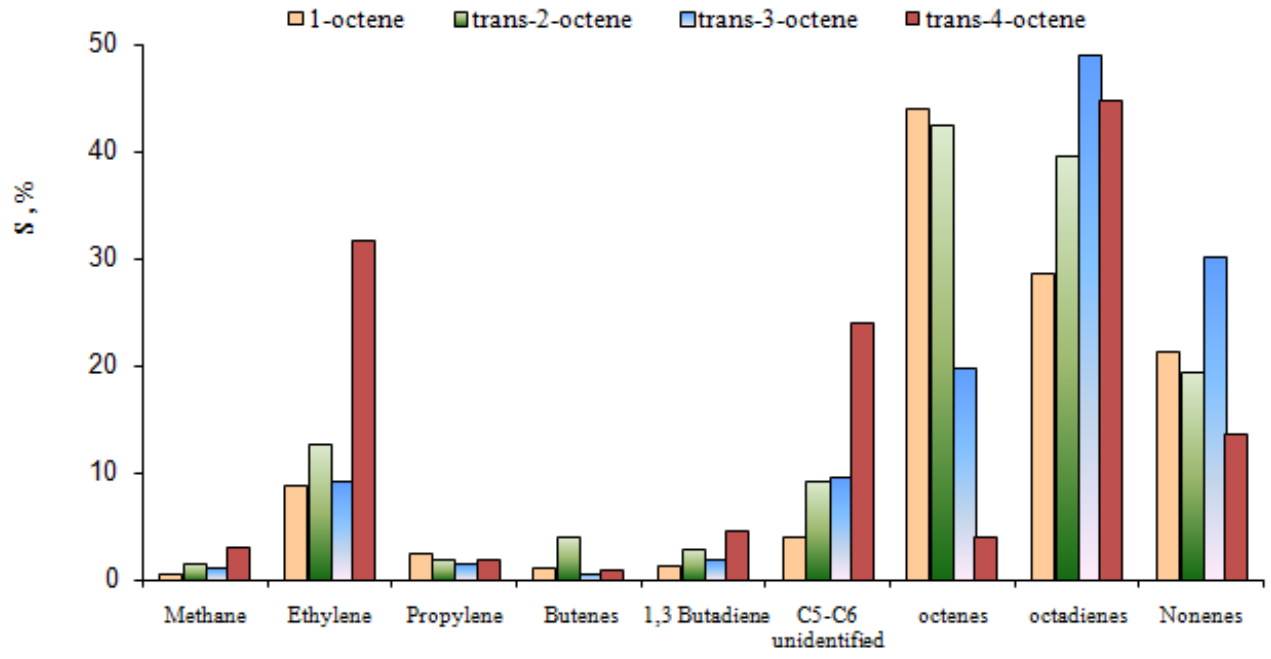

Figure 9: Primary cracking selectivity of products for feedstock in study

The primary selectivity can be defined as the distribution of products resulting from primary reactions. As verified in Figure 9, the majority of primary products obtained for all unsaturated hydrocarbons in study are ethylene, C_5-C_6 unidentified hydrocarbons and C_8-C_9 compounds. The heaviest products may result from isomerization, hydrogen transfer (in particular hydrogen abstraction to form octadienes) and addition reactions, while the lightest products are formed by radical mechanisms.

It is clear from Figure 9 that the primary selectivity of ethylene production is much higher in trans-4-octene pyrolysis (about three times higher) than in other feedstock pyrolysis. Trans-2-octene is the second raw-material that produces more ethylene in primary reactions and the other two samples have similar selectivity.

Observing propylene production, it is possible to say that it is practically independent of the double bond in the hydrocarbon chain because selectivity is slightly decreasing from 1 to 4 position.

There is substantially higher selectivity to butenes in trans-2-octene pyrolysis than in other feedstock pyrolysis.

For 1,3-butadiene the selectivity is greater than for methane, but with the same tendency. The selectivity has the highest value for steam cracking of trans-4-octene and the smallest for 1-octene.

Analyzing the production of C_5-C_6 unidentified hydrocarbons, it is obvious that the selectivity to them increases when the position of the double bond is higher in the hydrocarbon chain (first to fourth position).

The opposite behavior is observed when analyzing the formation of other octenes than the starting octenes. This indicates that the isomerization occurs strongly in first position and decreases in further position in the hydrocarbon chain.

Formation of octadienes occurs with more intensity for trans-3-octene and less intensity for 1-octene. Although it can occur by molecular reactions (dehydrogenation) that is encouraged by forming conjugate double bond system, it is more likely that the preference can be explained by common radical mechanism, namely by the inability of trans-3-octen-2-yl radical to perform C-C bond β-scission compared to the 1-octen-3-yl radical.

Great selectivity to nonenes for unsaturated hydrocarbons with 8 carbon atoms pyrolysis was unexpected because the main primary reactions are scission and isomerization and this kind of reactions form products with the same or less carbon atoms. Molecules with more carbon atoms than the starting material are formed by addition of two radicals. The feedstock with less addition reaction is trans-4-octene while trans-3-octene has the highest selectivity. It is also necessary to note that the formation of nonenes was proved by the GC-MS identification of products, but their reported amount may be deviated by interference with octatrienes that exhibit similar retention times in the system with multicolumn separation of products.

More extensive analysis will be made later when reaction pathways will be analyzed.

Since most radicals are formed during the propagation step, by withdrawing hydrogen from the starting compound, it is necessary to know the C-H bond dissociation energies (BDE) to determine which bonds will split more easily and consequently, which radicals will possess the higher probability of formation. The C–H bond dissociation energies for the hydrocarbons under study are shown in the Table 10.

Table 10: C-H bond dissociation energies in unsaturated hydrocarbons

Compound	Link type	BDE (kJ.mol^{-1}) [16]
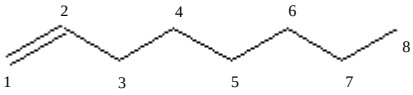	$C_1 - H$	465.3
	$C_2 - H$	429.9
	$C_3 - H$	348.9
	$C_{4=5=6=7} - H$	410.0
	$C_8 - H$	414.2
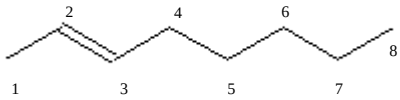	$C_1 - H$	356.8
	$C_{2=3} - H$	429.9
	$C_4 - H$	342.7
	$C_{5=6=7} - H$	410.0
	$C_8 - H$	414.2
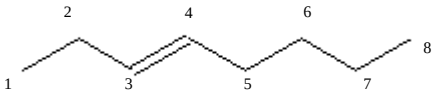	$C_1 - H$	419.2
	$C_{2=5} - H$	348.8
	$C_{3=4} - H$	429.9
	$C_{6=7} - H$	410.0
	$C_8 - H$	414.2
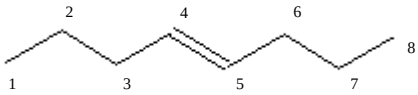	$C_{1=8} - H$	419.2
	$C_{2=7} - H$	410.0
	$C_{3=6} - H$	348.8
	$C_{4=5} - H$	429.9

The values of BDE presented above were almost exclusively obtained indirectly by analogy with bond energy dissociation of other molecules containing the same structural elements because there were no values available in literature for all links. Only for C-H bonds, in β-position to the double bond, the value was obtained directly.

For example, in 1-octene molecule C_1 – H dissociation energy was considered the same that for ethylene, because ethylene was the molecule found with two hydrogen atoms linked to one carbon with a double bond. In literature, is possible to find the radical formation energies of $CH_3\dot{C}=CH_2$ and $CH_3CH=\dot{C}H$. The difference of these energies is the same that between $CH_2=\dot{C}C_5H_{10}CH_3$ and $\dot{C}H=CHC_5H_{10}CH_3$ being possible to calculate C_2 – H bond energy dissociation subtracting this difference to C_1 – H energy. It was also take in consideration that carbons further than β-position to double bond has the same dissociation energy ($C_{4=5=6=7}$ – H) except for the primary hydrogen in 8-position, in the carbon chain, that the value assumed was the same of hexane.

For other substances similar analogy was made.

It is usual to consider that the primary cracking reactions run chiefly by pseudo-first-order, and under Arrhenius law [30]:

$$k = A_0 \cdot e^{\left(\frac{-E_d}{RT}\right)} \tag{4.1}$$

where, k is the reaction rate coefficient, A_0 is the pre-exponential factor, E_d is the dissociation energy, R is the gas constant and T is the absolute temperature (in Kelvin). Therefore, the reaction rate can be obtained through the equation (4.2):

$$r = k \cdot C^n \cdot n_H \tag{4.2}$$

in which k is the reaction rate coefficient, C is concentration of the feedstock, n is the reaction order and n_H is the number of hydrogen attached to the carbon atom with the same bond energy dissociation.

One way to predict the radical formation it is by calculating the ratio between the splitting rate of the bond (which breaks to form the radical) and the sum of all possible C - H dissociation energies in the molecule:

$$\frac{r_i}{\sum_{i=1}^{8} r_i} = \frac{e^{\left(\frac{-(E_d)_i}{RT} n_{H_i}\right)}}{\sum_{i=1}^{8}\left[e^{\left(\frac{-(E_d)_i}{RT}\right)} \cdot n_{H_i}\right]} \tag{4.3}$$

The radical formation occurs by hydrogen abstraction, like said above. In unsaturated hydrocarbons the double bond strengthens the ties of the carbon linked to the double bound and weakens the subsequent bounds in the hydrocarbon chain, because of the increased stability of allyl-type radical. Therefore, the hydrogen bond which has the highest probability to split is the one in allyl-position to the double bond. The probability of forming an allyl-type radical is close to 100 % at 620 °C. In following figures is shown the radicals formed and the radical isomerization reactions that could occur in all feeds.

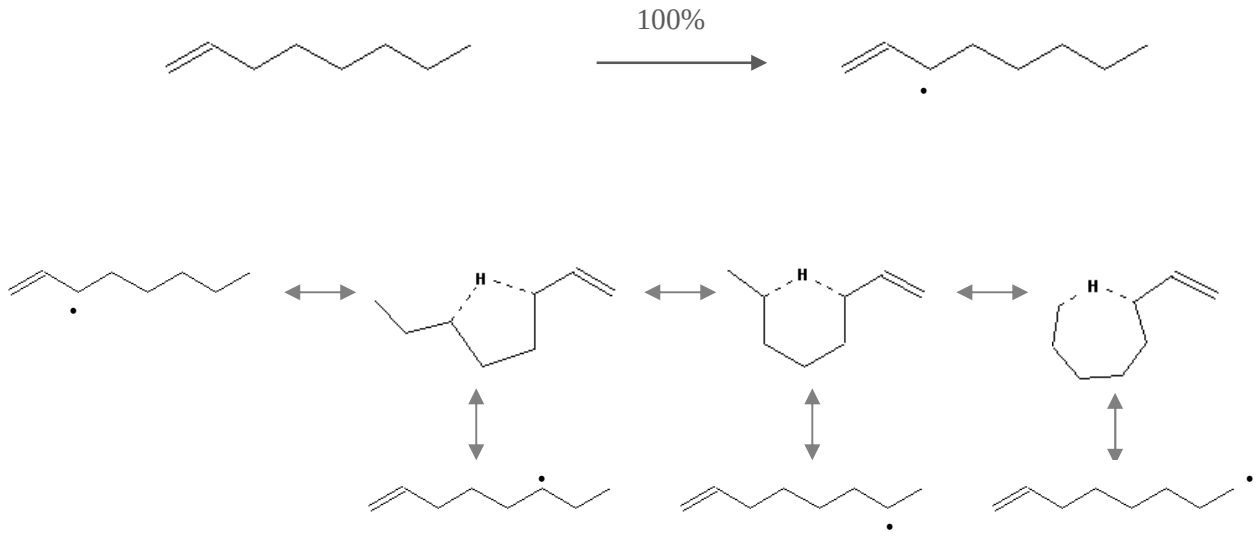

Figure 10: Scheme of radical formation probability and isomerization paths of 1-octene

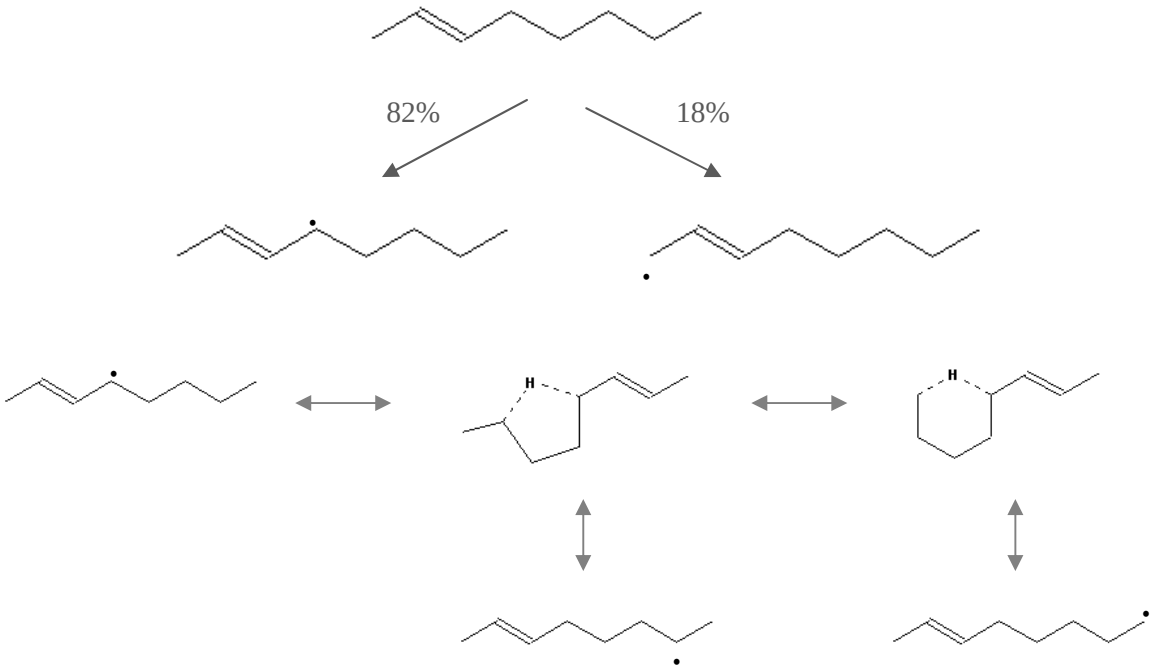

Figure 11: Scheme of radical formation probability and isomerization paths of trans-2-octene

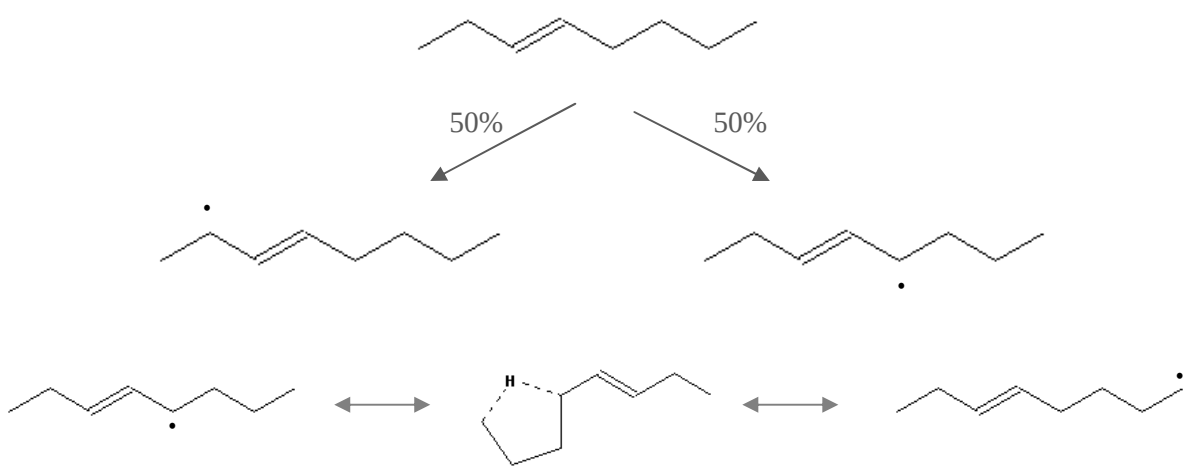

Figure 12: Scheme of radical formation probability and isomerization paths of trans-3-octene

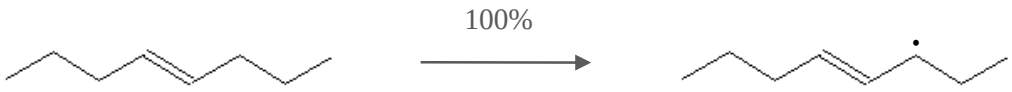

Figure 13: Scheme of radical formation probability of trans-4-octene

The primary selectivities to other octene isomers obtained using experimental data (Figure 9) are in good agreement with the principle of isomerization of radicals. As represented in the figures above, the possibility of isomerization decreases from 1-octene to trans-3-octene and in trans-4-octene there is nearly no isomerization at all because the minimum ring permitting feasible isomerization is the ring with four carbon atoms (1-5 isomerization). The percentages of isomerization reactions of radicals considered are related to values of primary selectivities of octenes obtained experimentally.

In order to analyze the reaction pathways, it was taken in consideration that the primary cracking reactions run chiefly by radical mechanisms like described above in section 2.1.1. Bonds in β-position to unmatched electrons are the weakest in hydrocarbon chain and consequently, the most common splitting reaction is β-scission of C - C bonds. β-scission of C-H bond can happen also, but with less frequency, because C-H bonds has higher bond dissociation energies than C - C bonds, about 100 $kJ.mol^{-1}$ more [16].

The reaction schemes of primary cracking by radical mechanism are represented below, in following figures:

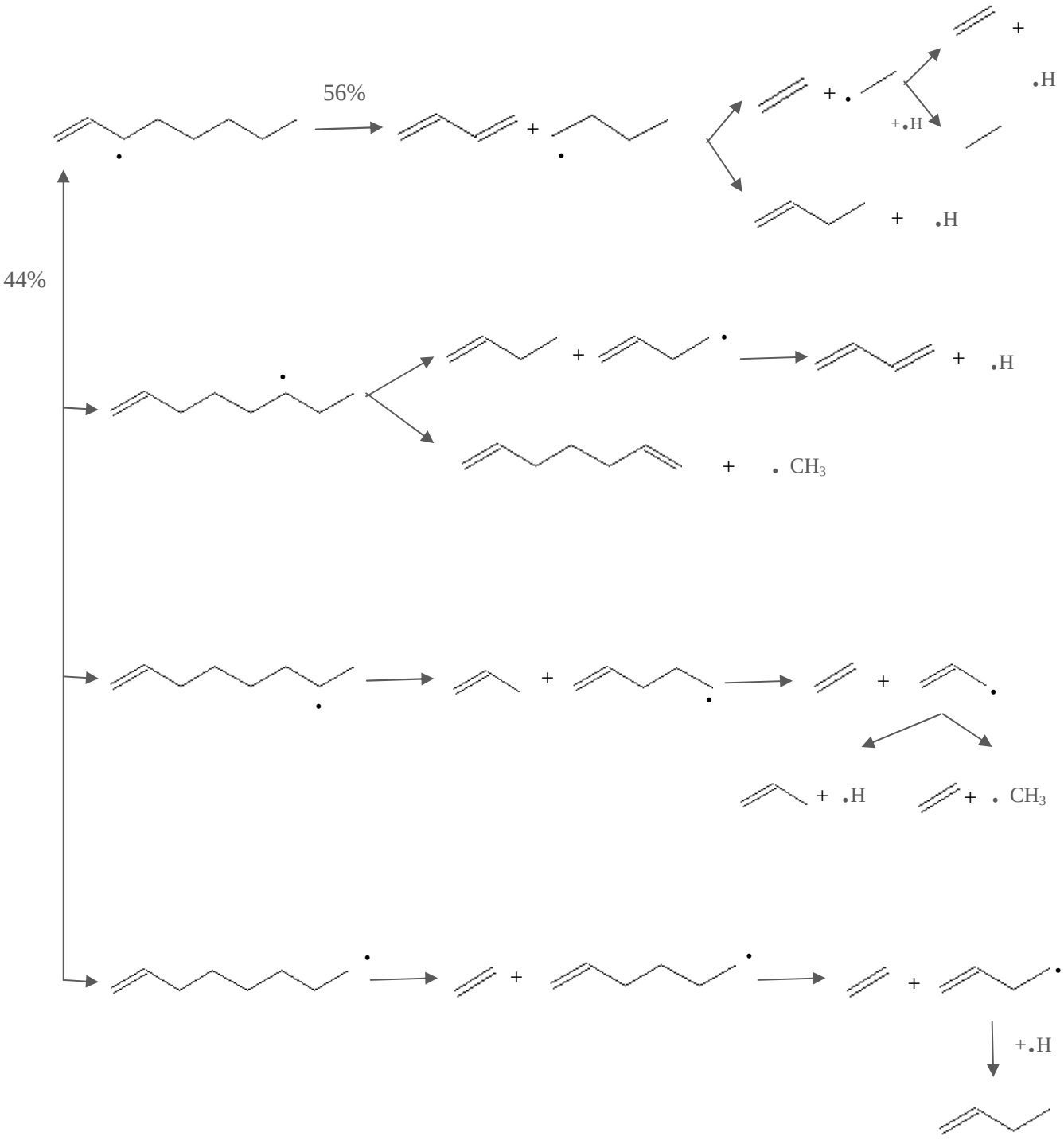

Figure 14: Scheme of primary pyrolysis reactions of 1-octene

From 1-octene the only radical formed by hydrogen abstraction, calculating the probabilities with equation (4.3), is 1-octene-3-yl. The pyrolysis of this radical originate mainly 1,3-Butadiene, ethylene and 1-Butene.The other radicals presents appear because of radical isomerization from 1 to 4,5 and 6 position. The rate of isomerization assumed was the primary selectivity of octenes and it is about 44%, Table 6. Isomerization leads also to propylene and 1,7-heptadiene production besides the compounds formed from 1-octene-3-yl and mentioned above. Methyl radical could accept one hydrogen atom to produce methane or participate in addition reactions with bigger molecule forming heavier compounds.

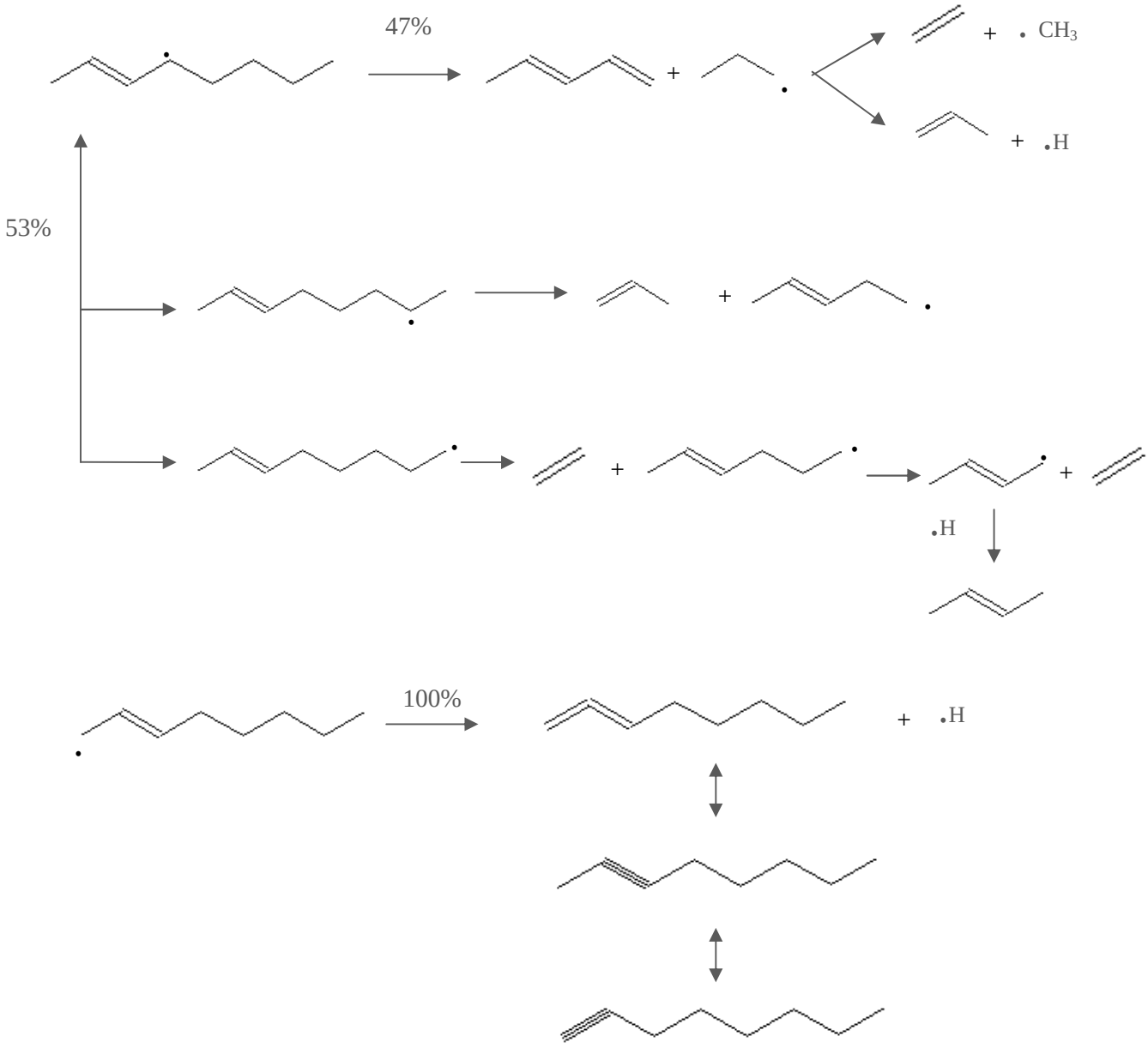

Figure 15: Scheme of primary pyrolysis reactions of trans-2-octene

As shown in Figure 11, trans-2-octene can form two different radicals by hydrogen abstraction. The most frequent is trans-2-octene-4-yl (82%) which can isomerizes from 1 to 4 and 5 position. Observing the figure above, it is possible to see that from it, radical mechanism reactions can explain the production of 2,4–pentadiene, ethylene and propylene. The rate of isomerization is 53% (corresponding to 42%, which is octenes' primary selectivity) forming as well as ethylene and propylene, 2-butene and 2-penten-5-yl. This radical should stabilize by merging with methyl or hydrogen or by acting like a radical in hydrogen abstraction reaction.

Trans-2-octene-1-yl can be formed with 18% of probability in trans-2-octene thermal cracking. By means of β-scission of a C-C bond this radical tend to produce a very unstable molecule, 1,2-octadiene, which easily isomerizes to 2-octyne or to 1-octyne. These two isomers with triple bond are very reactive and can participate in addition reactions forming heavier compounds.

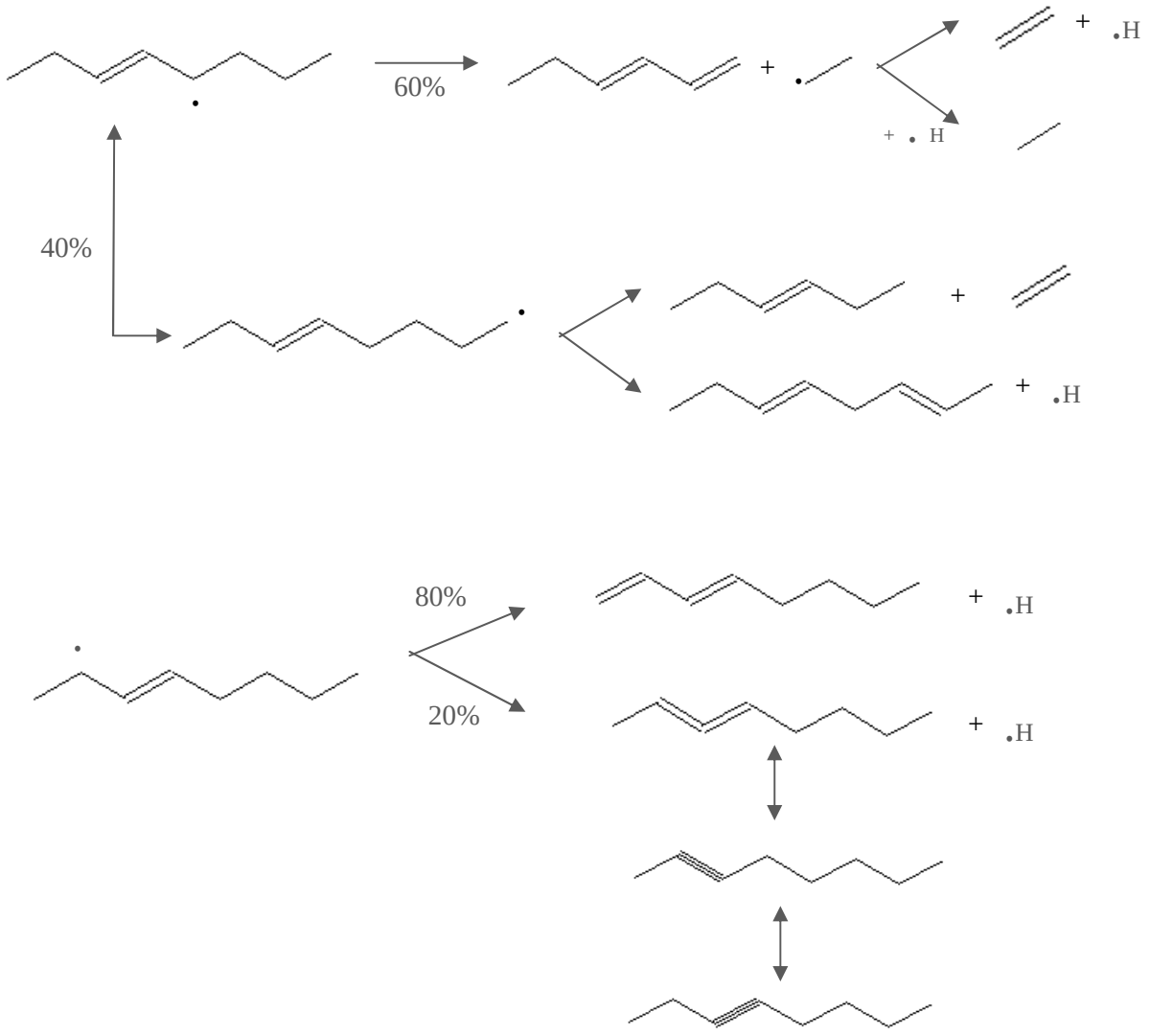

Figure 16: Scheme of primary pyrolysis reactions of trans-3-octene

By hydrogen abstraction, in the allyl-position to the double bond, trans-3-octene forms two radicals with same probability, Figure 12. Only trans-3-octene-4-yl can isomerize (from 1 to 4-position). Looking to Figure 16, it is possible to see that this radical can originate C_6 with one and two molecules and also ethylene, ethane and 3,6-octadienes.

The other radical with unpaired electron in second position of hydrocarbon chain only produces octadienes by β-scission of the C-C bond. The octadiene less formed (20%) is a very unstable molecule, 2,3-octadiene, which easily isomerizes to 2-octyne or to 3-octyne. Like octynes seen in trans-2-octene reaction pathways, these two isomers with triple bond are very reactive and can participate in addition reactions forming heavier compounds, such as nonenes.

Trans-4-octene has a symmetric hydrocarbon chain and only forms trans-4-octene-3-yl radical. This radical do not isomerizes because the saturated part of the hydrocarbon chain is not large enough to form at least an 4-membered ring. So, by radical mechanism trans-4-octene steam cracking only produces as primary products 1,3-octadiene and methyl radical which can originate methane, as shown in following scheme of reaction pathway:

Figure 17: Scheme of primary pyrolysis reactions of trans-4-octene

At least, for trans-4-octene, it is obvious, looking to figure above and to the primary selectivities, that the radical mechanism is insufficient to explain the formation of primary cracking products. Experimentally trans-4-octene is the feedstock which produces more ethylene and by radical mechanisms is impossible to form this molecule.

Corrections in reaction mechanisms

Two possible ways to explain the results obtained that obviously do not occur directly by radical mechanisms are allyl type radical delocalization [31] and retro-ene reactions[32].

Hydrogen abstraction of linear unsaturated hydrocarbon leads to formation of allyl radical. The allyl radical is a small conjugated system with unpaired electrons and is the molecule classically used to exemplify resonance theory. This theory explains that when there are unpaired electrons near to the double bond them can switch in the hydrocarbon chain like is shown in figure below:

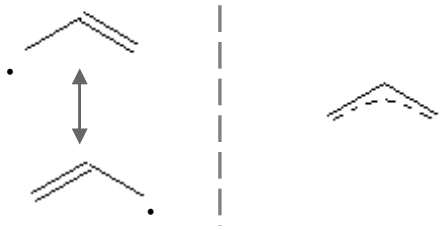

Figure 18: Scheme of allyl type radical delocalization

This radical delocalization can occur in all feedstock in study because all radicals formed are in allyl-position to double bond except those formed by isomerization reactions.

For example radical trans-4-octene-3-yl is in equilibrium with trans-3-octene -4-yl:

Figure 19: Allyl radical type radical delocalization in trans-4-octene

With the existence of this radical it is now possible to explain by radical mechanisms the production of ethylene C_6 hydrocarbons with one and two double bonds and octadienes.

Analogical discussion can be made for other molecules.

The other type of reaction considered is retro-ene reaction. The mechanism of this reaction is similar to radical isomerization from 1 to 5 position, but in this type what happens is an 1 to 5 hydrogen shift followed by scission of C-C bond in β-positon to unpaired electron in the transition state.

For a better viewing of the mechanism, is shown in Figure 20, retro-ene reaction in trans-3-octene molecule.

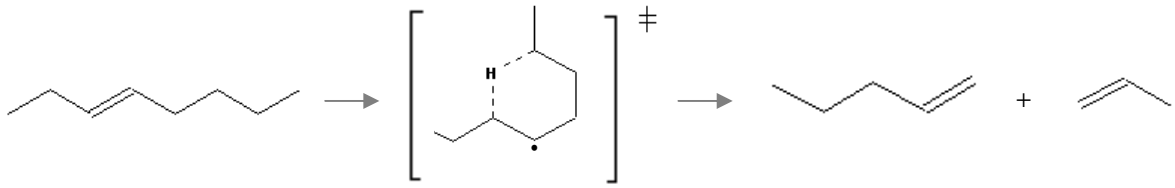

Figure 20: Retro-ene reaction in trans-3-octene

Similar reactions can happen with the other feedstocks. Retro-ene reaction of 1-octene leads to formation of same compounds as trans-3-octene, such as 1-pentene and propylene. Trans-2-octene only forms 1-butene while trans-4-octene can produce 1-hexene and ethylene by this means.

4.2 Artificial Neural Network Simulations

Like stated above in chapter 2.3, one of the possible ways to predict the products obtained at high conversions (high temperatures) is to train an artificial neural network using experimental data resulted from primary cracking experiments at low temperatures as inputs and product yields obtained at high conversion experiments as outputs. If there is a sufficient and reliable experimental data and the network is well trained, it provides an adequate fit and is capable to predict the desired results.

Though the benefits of predicting one type of experimental results from another are questionable, it is also possible to scale-up the laboratorial data in industrial practice, using as outputs product yields, obtained in industrial conditions and possibly the temperature of reaction mixture in the reactor and the steam-feedstock ratio by the same means. If the network created is able to predict the product yields, only doing laboratorial experiments at low temperatures will it improve the performance of technological processes in order to achieve savings in energy to tune the production and to protect the environment. The feasibility of developing such a neural networks model is better to be tested on model laboratory data at first, since there is better control of experimental errors and consistent set of experimental data can be obtained more easily.

The experiments at high temperatures were carried out to train a network able to predict pyrolysis product yields, as shown in the following table:

Table 11: Product yields resulting from the pyrolysis of feedstocks at 810 ºC

Feed	**1-octene**	**trans-2-octene**	**trans-3-octene**	**trans-4-octene**
Products		**y** (wt.%)		
Methane	4.1	13.8	9.8	7.7
Ethane	1.1	6.0	4.6	2.7
Ethylene	48.5	36.3	45.0	48.6
Propane	0.3	1.0	1.8	0.8
Propylene	21.6	8.0	7.7	10.5
Acetylene	0.5	0.7	0.6	0.7
iso-Butane	0.5	0.1	0.1	0.2
Propadiene	0.0	0.1	0.4	0.1
trans-2-Butene	9.2	2.1	1.9	3.5
1,3-Butadiene	9.4	17.6	13.9	16.0
C_5-C_6 unidentified	2.5	5.9	4.6	3.8
Benzene	1.6	5.8	6.4	3.7

From Table 11 it is possible to see that ethylene is produced almost in the same quantities when 1-octene, trans-3-octene and trans-4-octene. When trans-2-octene is cracked at high temperatures ethylene yields only achieve 36.3%. For the most valuable byproduct, propylene is shown in same table that the feedstock which produces more is 1-octene.

The results obtained experimentally are not enough to train the network adequately, because they are not many and they are only from pyrolysis of linear unsaturated hydrocarbons. Therefore, the training set was supplemented, by the experimental data, from pyrolysis of saturated and branched hydrocarbons measured some time ago, using the same equipment. These values are presented in Annex C.

A 14-element numerical vector which corresponds to carrier-gas flow, temperature, conversion and the most significant mass product yields from low conversion pyrolysis was used as input, whereas the yields of methane, ethylene and propylene at high temperature experiments, were selected as outputs (Figure 21).

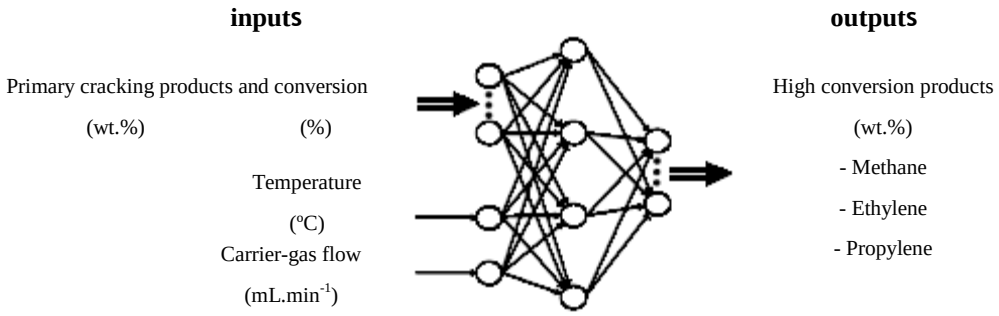

Figure 21: Scheme of neural network model used

The behavior of an ANN depends on both the weights and the input-output functions (transfer functions) that is specified for the units. For the hidden layer the transfer function used was the hyperbolic tangent sigmoid transfer function (tansig), good to approach non-linear terms and for the output layer the transfer function used was the hard limit transfer function (purelin) because if linear output neurons are used the network outputs can take on any value, which do not happen if sigmoid neurons are used. The neural network should be trained in order to adjust the weights

of each unit in such a way that the error between the network outputs and the target outputs is reduced, i.e., minimize the feedforward default performance function – mean square errors.

The training function chosen was the Levenberg Marquardt backpropagation (trainlm) because, besides the fact that normally it achieves good results, it is faster than the other possible training functions.

To simulate and train the network a code (annex B) was developed using an application in MATLAB software called Neural Network Toolbox present. Normalize was an important step, because all the inputs need to be values between 0 and 1 to transfer functions can be used. After simulation the values were denormalized in order for the outputs generated to have the real values. To make different simulations only few parameters, like goal and training function, were changed from the code base.

The first simulation done was simple Levenberg-Marquardt using all data available as training set, i.e., without using validation set. The results obtained of mean square errors for 10, 100 and 1000 iterations are present in the column graph in figure below:

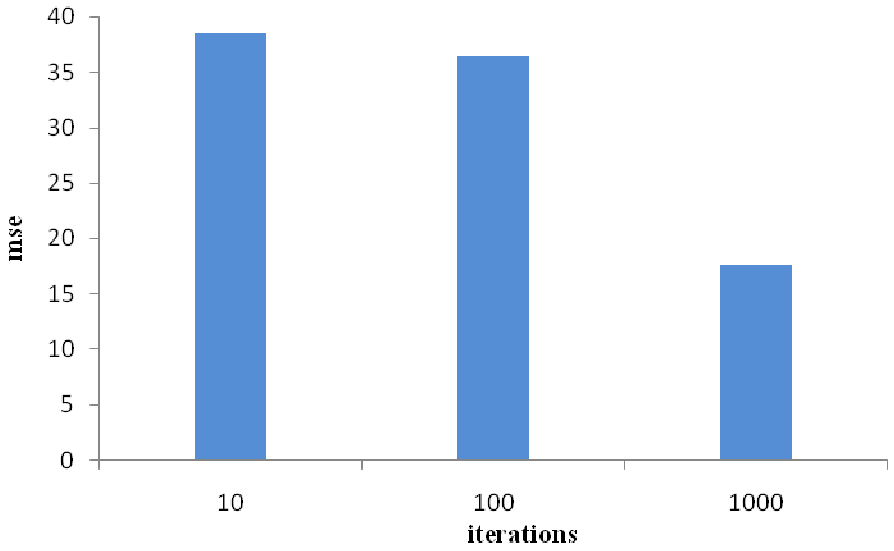

Figure 22: Mean square error for ANN training without validation

It is possible to see that the error obtained, even when 1000 iterations cycle run, is very large. It is also known, from literature, that it is important to improve generalization in order to prevent that the network memorize the training examples instead of learning new situations (data overfitting). To avoid this problem the data used was divided into two sets: training (80%) and validation (20%).

Two methods were used to improve generalization: Bayesian regularization and early stopping.

In Bayesian regularization method, it was necessary to change the training function trainlm to trainbr function, which determines the optimum values of weights and biases automatically.

In early stopping, the validation set of data is included to obtain the validation error. The validation error has a decreasing tendency in the initial phase of training, but when the network starts to overfit the data, the error on the validation set, starts to rise. As soon as it happens, the training stops and the weights and biases take the value achieved in the minimum value of validation error.

The network was trained with these two methods choosing three, four or five nodes in the hidden layer.

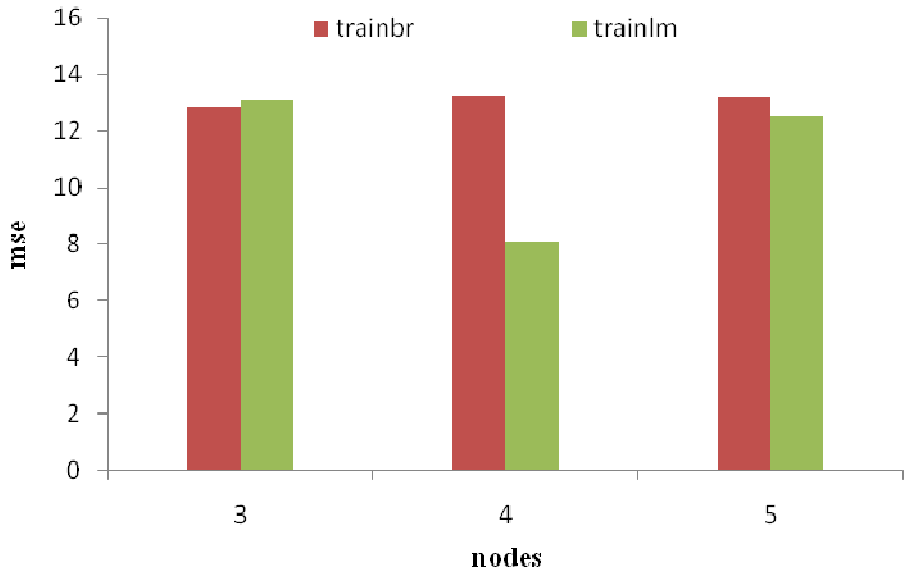

Figure 23: Mean square error using Bayesian regularization and early stopping in Levenberg-Marquardt algorithm, with 100 iterations

Observing Figure 23 it is possible to see that using three or five nodes in the hidden layer it has almost the same results for both methods, but using four nodes, Levenberg -Marquardt with validation the result is significantly better when compared with Bayesian regularization in same conditions.

Another way to train the network is by setting the network goal to an optimal value. This procedure is made manually, which is not very reasonable in industrial work because it could take too much time to set the best goal.

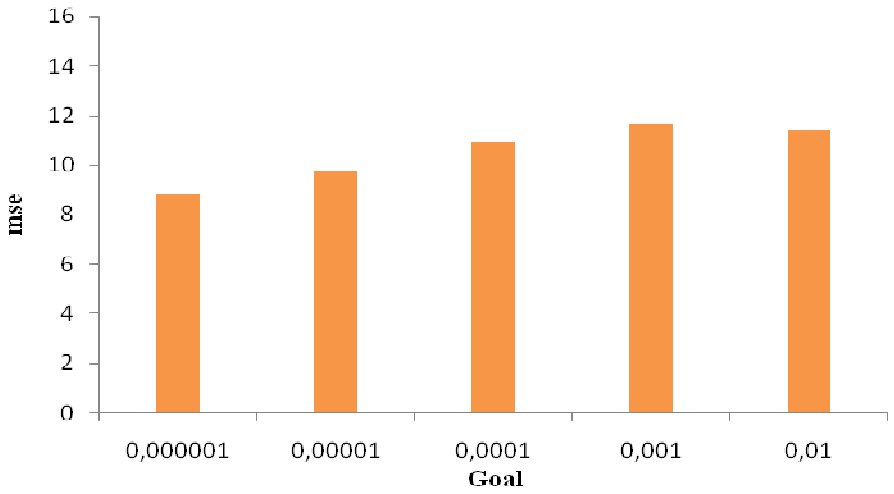

Figure 24: Mean square error for goal settings in a network with 4 nodes in hidden layer with 100 iterations

As shown in column graph represented in Figure 24, the best results were obtained when the goal was setted to 0,000001. To reach best network training it was necessary to make changes in the goal near 0,000001 to get the optimum goal and the optimal values for network parameters.

With the aim to compare all the simulations done in neural network training it is presented in the next figure how the performance function differ in all simulations when the simulation runs one hundred times.

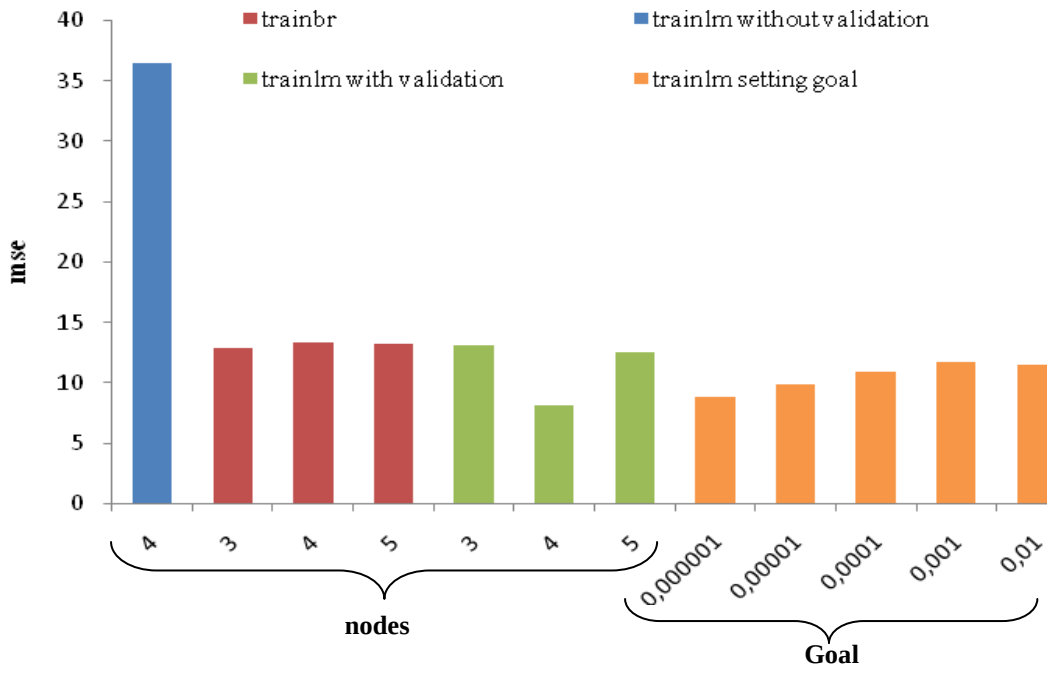

Figure 25: Mean square errors in network training

Looking to the picture above it is evident that the best network trained was the Levenberg-Marquardt with four nodes in the hidden layer when improve generalization is made by early stopping while the worst result was obtained when there is no validation in the network.

Other concern in network training is to know how many times the network should run to learn adequately how to react to a new input. After chosen the best method to train, the network was trained from one to ten thousand iteration cycle. The performance function obtained is shown in Figure 26.

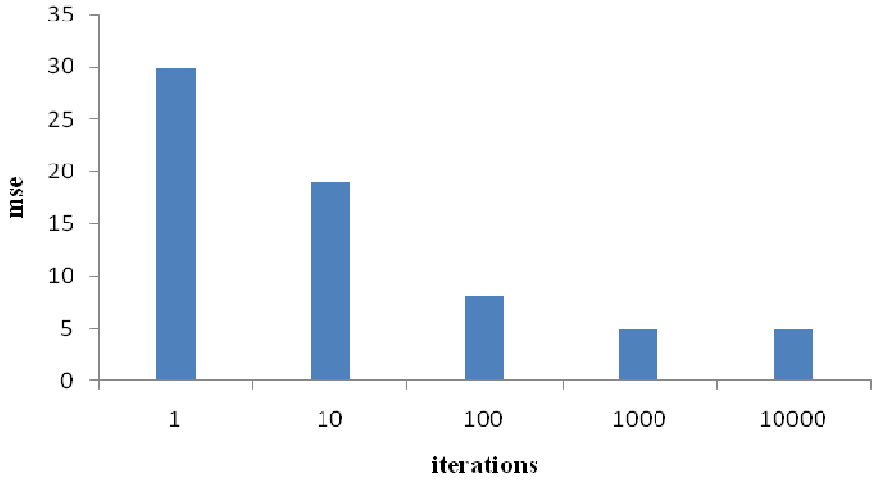

Figure 26: Mean square errors in Levenberg-Marquardt with validation for different number of iterations

Although the best performance obtained was running the network ten thousand times, achieving mean square error value of 4.9710, the optimum number of iteration is one thousand because the mean square error is very similar (4.977) and the simulation takes much less time than for ten thousand iteration simulation, like ten times less.

The outputs obtained in the selected neural network, when the network was training one thousand times with Levenberg-Marquardt algorithm with validation, are presented in following figures:

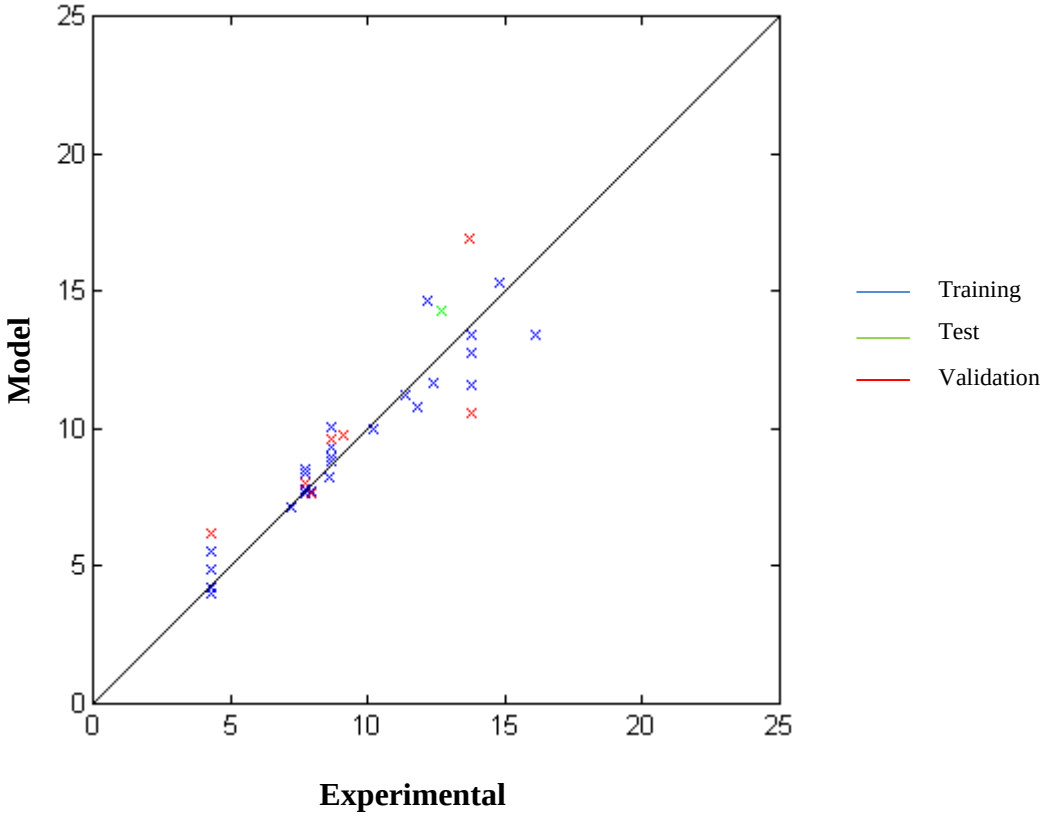

Figure 27: Simulation results for methane

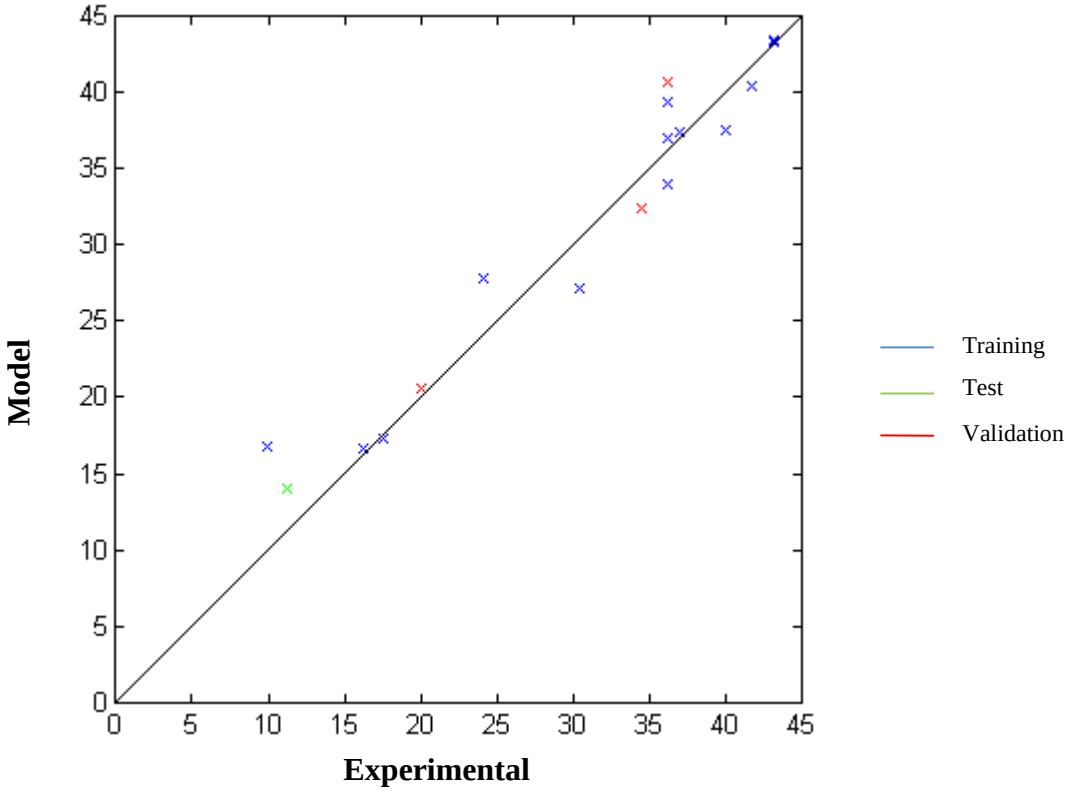

Figure 28: Simulation results for ethylene

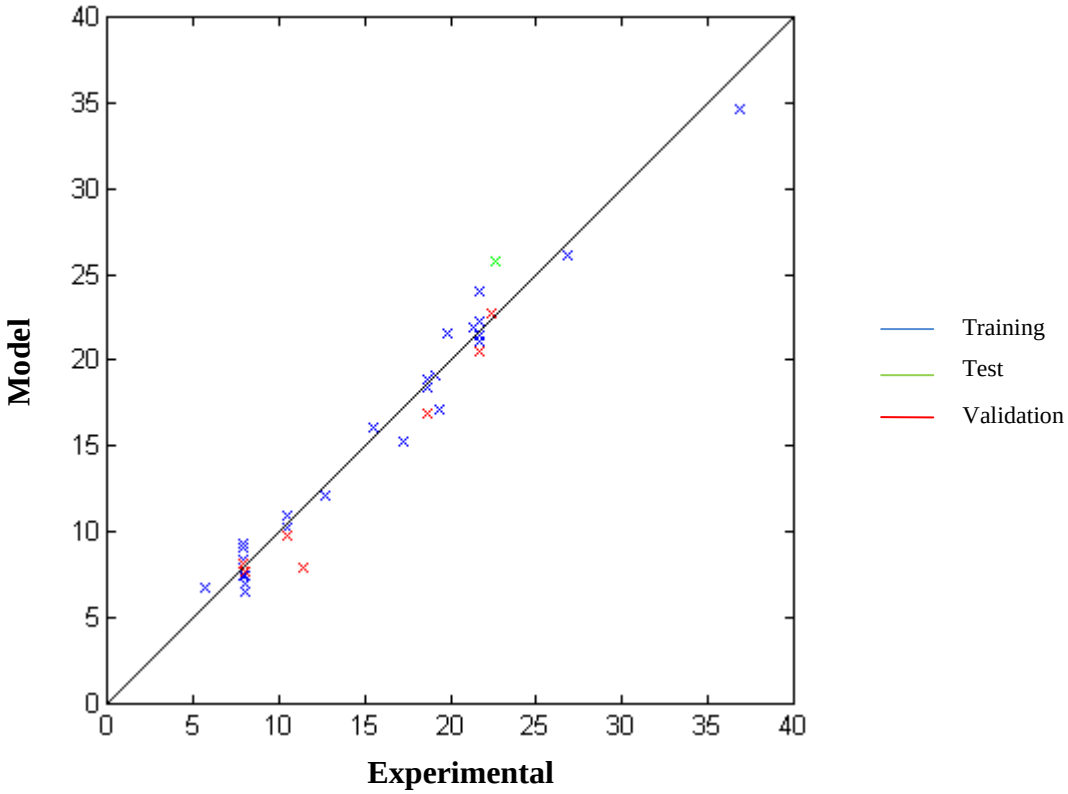

Figure 29: Simulation results for propylene

Observing the previous pictures it is possible to see that the results are quite good because they are distributed near the diagonal line. When the results are on the line, it means that the experimental data and the data provided with the model are in perfect agreement. To improve the quality and reliability of output results provided by the neural network more experimental data and from different types of hydrocarbons should be added in the neural network training.

The best results obtained were for propylene because experimental outputs are in fact very close to values given by neural network simulation, as shown in Figure 29.

5 Conclusions

Nowadays, the study of the relation between thermal cracking selectivity and feedstocks structure is very important because it can predict the product composition and decide if the ethylene production is economically profitable by thermal cracking of one specific type of raw material or not. It is also possible to find out if the use of particular waste hydrocarbon stream in refineries (which need to be recycled) is advantageous or not without testing in industrial plants, avoiding unnecessary investments and protecting the environment. Being a part of a bigger project supported by the Grant Agency of Czech Republic, the study made is important because it will contribute to get a broad background of feedstock structures and will help to understand pyrolysis mechanisms.

One of the aims of the project was to study primary cracking reactions in a group of four linear unsaturated hydrocarbons with the same molecular weight, in which the difference is the position of the double bond in the hydrocarbon chain. The C-C and C-H bond scissions were studied based in bond dissociation energies and in the rate of bond scission calculated by Arrhenius Law, proving that the bond which split easily is the C-C bond in β-position to unpaired electrons.

Comparing experimental data with analysis of reactions pathways it can be concluded that the primary cracking reactions run mostly by radical mechanisms, except in trans-4-octene pyrolysis. Trans-4-octene was the hydrocarbon which produced more ethylene as a primary product with 31.6% of selectivity while for the other feedstocks the primary selectivity of ethylene was about 10%. This was unexpected because the bond dissociation energies analysis indicated only formation of such radicals, the β-scission of which only produces octadienes and methane (and C_7). The production of lightest products, like ethylene, in trans-4-octene thermal cracking can be explained by allyl type radical delocalization which effectively causes the radical isomerization around the double bond or by retro-ene reactions.

For propylene production, the most valuable byproduct in ethylene production, the best primary selectivity achieved was for 1-octene with 2.6% of selectivity.

Isomerization reactions theory are in good agreement with experimental data because like demonstrated, in theory the possibility of isomerization, decreases from 1-octene to trans-3-

octene and in trans-4-octene there is no isomerization and experimental data given by octenes selectivity followed the same trend.

To predict the relationship between selectivities of primary cracking and product yields in high conversion cracking was developed an artificial neural network. The results obtained are not very realistic because the range of inputs in the network does not include all type of structures of hydrocarbon.

With the experimental data used, in backpropagation network, trained using Levenberg-Marquardt function, the best results obtained were for a network with two layers (with four nodes in the hidden layer), when improving generalization was performed by early stopping for 1000 iterations.

6 Assessment of Work

6.1 Goals Achieved

In this research the bond position effect in a broad linear unsaturated hydrocarbon in thermal cracking reactions mechanisms was studied successfully. It was also performed a neural network with data available, but it was proved that the network was poor because of the lack of experimental data used to train the network.

6.2 Limitations and Future Work

This work is part of a bigger project sponsored by Grant Agency of Czech Republic. The working team is constituted by members of Organic Department in ICT and Chemopetrol and the project is in the beginning and will be completed during the next three years. The main limitations found were in the modeling part because the whole research is in the beginning and does not exists much experimental results to train a network obtaining optimal results. The lack of suitable data to train the network, with broad structure variability, was the main problem because the network is not capable of predict product yields for all feedstock possible.

7 References

[1]. http://www.bvt.umweltbundesamt.de/archiv-e/lvocbref-e.pdf, acessed on February 29th, 2008

[2]. Eisele, P., Killpack, R., (2005) "Propene", *John Wiley & Sons*, cap. 4

[3]. Meyers, A., (2004) "Handbook of Petrochemicals Production Processes", *McGraw-Hill Handbooks*, 3rd edition, cap.6.2

[4]. Herink, T., Fulin, P., Lederer, J., Belohlav, Z., (2001) "The kinetic model of thermal cracking for olefins production", *Oil & Gas Journal, **50***, pp. 461-473

[5]. Safrik, I., Strausz, P., (1996) "The thermal decomposition of hydrocarbons: Part 1. n-alkanes (C≥5)", *Research on Chemical Intermediates*, **22**, pp. 275-314

[6]. Trambouze, P., (2000) "Petroleum Refining – Materials and Equipment - Vol.4", *Editions TECHNIP*, 2nd edition

[7]. Starkbaumová, L., Belohlav, Z., Zámostný, P., (2005) *Primary reactions and products of hydrocarbon pyrolysis*

[8]. Albright, L., Crynes, B., Corcoran, W., (1983) "Pyrolysis: Theory and Industrial Practice", *Academic Press, **23***, pp.743

[9]. Sundara, K., Froment G., (1978) "Modeling of thermal cracking kinetics. 3. Radical mechanisms for the pyrolysis of simple paraffins, olefins, and their mixtures", *Ind. Eng. Chem. Fundam.*, **17**, pp. 174-182

[10]. Benson, S., (1968) "Thermochemical Kinetics", *John Wiley &Sons*, 1st edition, cap.5

[11]. Rice, F., (1931) "The Thermal Decomposition of Organic Compounds from the Standpoint of Free Radicals" *Journal of the American Chemical. Society **53***, pp.1959 - 1972

[12]. Rice, F., Herzfeld, K. (1934) "The Thermal Decomposition of Organic Compounds from the Standpoint of Free Radicals. IV –The Mechanism of some Chain Reactions", *Journal of the American Chemical. Society **56***, pp. 284 - 289

[13]. Vreven, T., Morokuma, K., (1999) "The accurate calculation and prediction of the bond dissociation energies in a series of hydrocarbons using the IMOMO (integrated molecular orbital+molecular orbital) methods" *Journal of Chemical Physics, **111***, p.8799

[14]. Feng, Y *et al*., (2004) "Homolytic C-H and N-H Bond Dissociation Energies of Strained Organic Compounds" *Journal of Organic Chemistry, **69***, pp.3129 - 3138

[15]. Zimmermann, H., Walzl, R., (2004) "Ethylene", *John Wiley &Sons*, caps.2 - 5.

[16]. Luo, Y. (2003) "Handbook of bond dissociation energies in organic compounds", *CRC Press*, cap. 3, 4, 11

[17]. Rice, F.O., Kossiakoff, A., (1943) "Thermal Decomposition of Hydrocarbons, Resonance Stabilization and Isomerization of Free Radicals" *Journal of the American Chemical. Society* ***65***, pp. 590 - 595

[18]. Belohlav, Z., *et al*, (2005) "Evaluation of pyrolysis feedstock by pyrolysis gas chromatography", *Petroleum Chemistry,* ***45***, pp. 118 - 125

[19]. http://www.organic-chemistry.org/namedreactions/diels-alder-reaction.shtm, accessed in 18 May 2008

[20]. Frech, K., (1970) "Cracking of Olefins" *US Patent* **3,529,032**

[21]. Dente, M., Pierucci, S., Ranzi, E., (1992) "New improvements in modeling kinetic schemes for hydrocarbon Pyrolysis", *Chemical Engineering Science,* ***47***, pp. 2629 - 2634

[22]. Clymans, P., Froment, G., (1984) "Computer generation of rate equations for thermal cracking of normal and branched paraffins", *Comp. Chem. Eng.****8***, pp.137 - 142

[23]. Joo, E., Lee, K.,. Lee, M., Park, S, (2000) "Cracker - a PC based simulator for industrial cracking furnaces", *Comp. Chem. Eng*, ***24***, pp. 1523 - 1528.

[24]. Belohlav, Z., Zamostny, P., Herink, T., Eckert, E., Vanek, T., (2005) "A novel approach for the prediction of hydrocarbon thermal cracking product yields from the substitute feedstock composition", *Chem. Eng. Technol.,* ***28***, pp. 1166 - 1176

[25]. Graupe, D., (1997) "Principles of Artificial Neural Networks: advanced series on circuits and systems", *World Scientific*, 1st edition, cap. 3, 4, 6

[26]. Fausset, L., (1994) "Fundamentals of Neural Networks: Architectures, Algorithms and Applications", *Prentice Hall*, 1st edition, cap 6.

[27]. Demuth, H., Beale, M., (1993) "Neural Network ToolBox for use with MATLAB", *The MathWorks* , 3rd edition, cap. 2,3 ,4 , 6

[28]. Sivanandman, S., Sumathi, S., Deepa, S. (2006), "Introduction to neural networks using MATLAB 6.0", *McGraw-Hill*, 2nd edition, cap.2, 5

[29]. Starkbaumová, L. (2005) "Experimentální a termodynamické studium chování cyklických-uhlovodíků při pyrolýze", Praha , VŠCHT Praha

[30]. March, J., Smith, M., (2007) "March´s advanced organic chemistry", *John Wiley & Sons*, cap. 2.3

[31]. Mo, Y., Lin, Z., Wu, W., Zhang, Q. (1996), Delocalization in Allyl Cation, Radical, and Anion", *J. Phys. Chem.,* ***100***, pp.6469 -6474

[32]. Fournet,R. *et al*., (2001) "The Gas-Phase Oxidation of n-Hexadecane", John Wiley &Sons, cap.3

Annex A

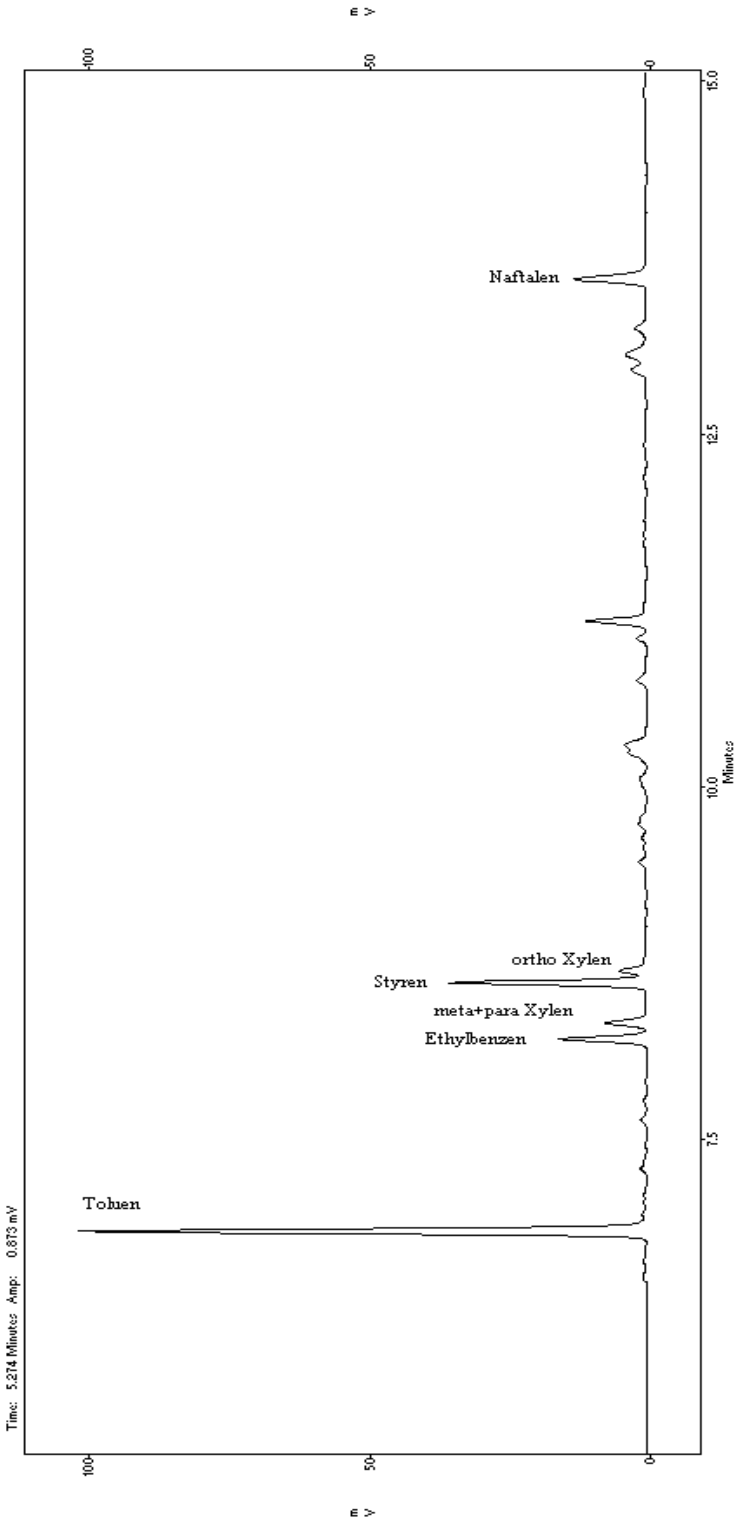

Figure A1: Spectrum of gaseous products of naphta pyrolysis as recorded with FID_1

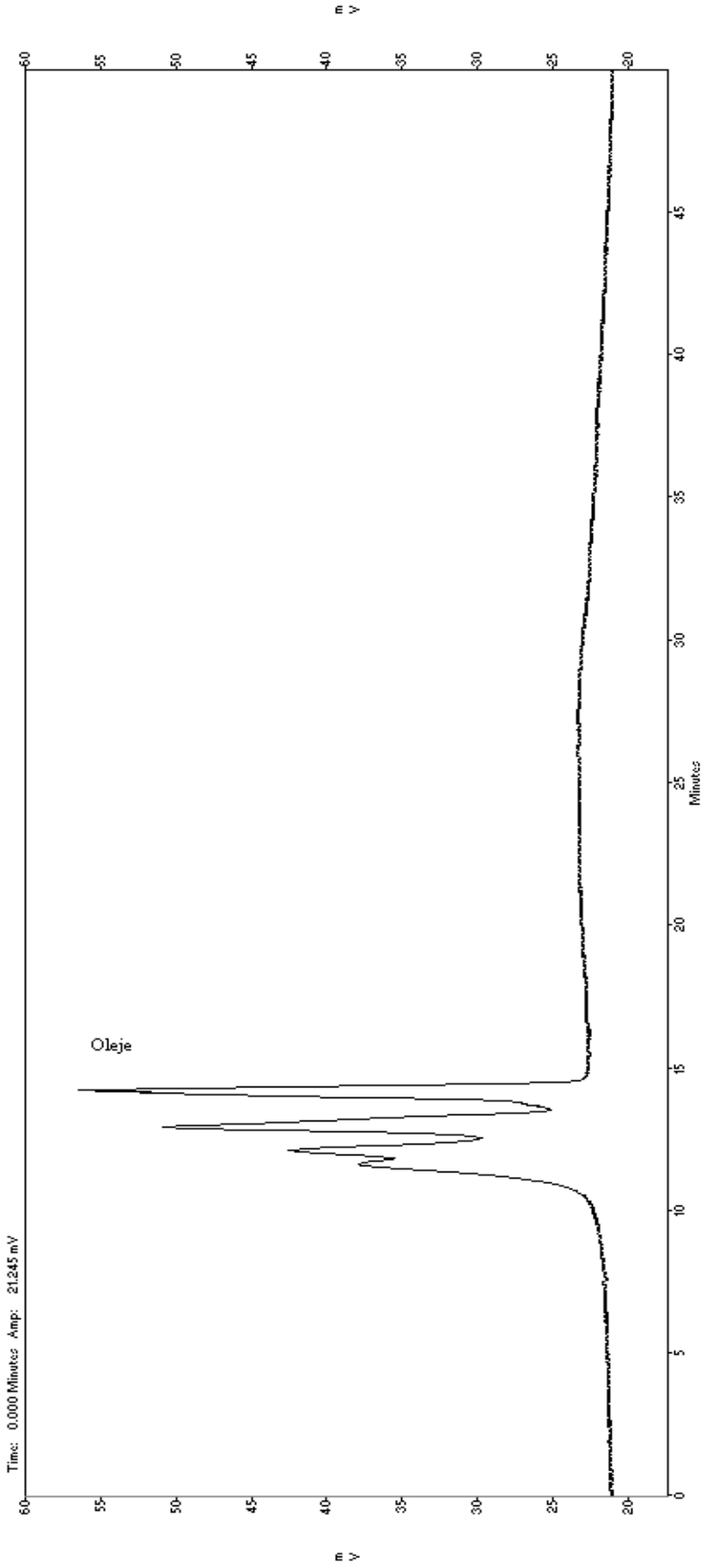

Figure A2: Spectrum of gaseous products of naphta pyrolysis as recorded with FID_2

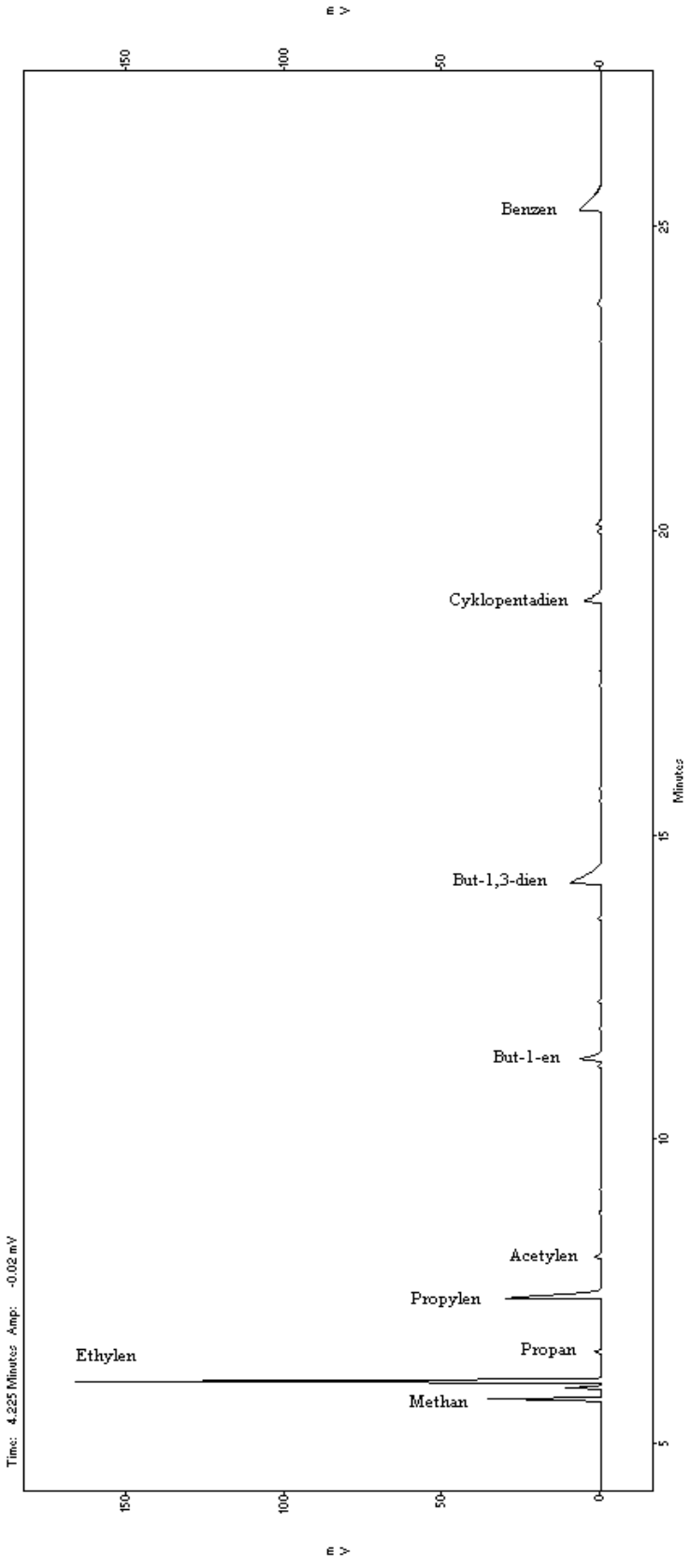

Figure A3: Spectrum of gaseous products of naphta pyrolysis as recorded with FID_3

Annex B

The code developed in MATLAB to train the network is presented below. Only changes in training function, goal and number of iterations were made in different simulations..

```
clear all; % Clears all data before new run

% Read table from Excel
[rawData,txtData] = xlsread('nn_data.xls');

% Parsing text part of data - Column headers and flags
IDs = txtData(1,2:end);
Names = txtData(2,2:end);

% taking only important rows
rawData = [rawData(1:3,:); rawData(5,:); rawData(7,:); rawData(12:15,:);
rawData(17,:); rawData(19:20,:); rawData(27,:); rawData(29,:); rawData(30,:);
rawData(32,:); rawData(34,:)];

% normalizing  data
rawMax = max(rawData')';
rawMin = min(rawData')';
rawSpan = rawMax - rawMin;

rawEMax = rawMax + rawSpan*0.25;
rawEMin = max(0,rawMin - rawSpan*0.25);
rawESpan = rawEMax - rawEMin;

NrawData = (rawData -
repmat(rawEMin,1,size(rawData,2)))./repmat(rawESpan,1,size(rawData,2));

% Input and output data
NiData = NrawData(1:(end-3),:);
NeData = NrawData((end-2):end,:);


% each 4th column will go to validation set
validFreq = 4;
tNames = [];
NliData = []; % Learning Data
NleData = [];
NviData = []; %Validation data
NveData = [];
NtiData = []; % Test Data
NteData = [];

for ii = 1 : size(NiData,2),
    if IDs{ii} == 'LV'
        if mod(ii,validFreq) == 0
            NviData = [NviData NiData(:,ii)];
            NveData = [NveData NeData(:,ii)];
        else
            NliData = [NliData NiData(:,ii)];
            NleData = [NleData NeData(:,ii)];
        end
```

```
    elseif IDs{ii} == 'L'
        NliData = [NliData NiData(:,ii)];
        NleData = [NleData NeData(:,ii)];
    elseif IDs{ii} == 'V'
        NviData = [NviData NiData(:,ii)];
        NveData = [NveData NeData(:,ii)];
    elseif IDs{ii} == 'T'
        NtiData = [NtiData NiData(:,ii)];
        NteData = [NteData NeData(:,ii)];
        tNames = [tNames Names(1,ii)];
    end
end;

mseBest = 1e8;

for ii = 1 : 1000


    % construct network
    net = newff(repmat([0 1],size(NiData,1),1), [4 3 ], {'tansig',
'purelin'},'trainlm');

    vv.P = NviData;
    vv.T = NveData;

    net.trainParam.epochs = 500;
    net.trainParam.goal = 0.0000;

    % training
    %net = train(net,NliData,NleData);
    net = train(net,NliData,NleData,[],[],vv);

    % Simulation
    NlsData = sim(net,NliData);
    NvsData = sim(net,NviData);
    NtsData = sim(net,NtiData);

    % Denormalize
    lsData = denormalize(NlsData,rawEMin,rawESpan);
    leData = denormalize(NleData,rawEMin,rawESpan);
    vsData = denormalize(NvsData,rawEMin,rawESpan);
    veData = denormalize(NveData,rawEMin,rawESpan);
    tsData = denormalize(NtsData,rawEMin,rawESpan);
    teData = denormalize(NteData,rawEMin,rawESpan);

    performance = mse(veData-vsData);
    if (mseBest > performance)
        mseBest = performance;
        netBest = net;
    end

end

net = netBest;

% Simulation
NlsData = sim(net,NliData);
NvsData = sim(net,NviData);
```

```
NtsData = sim(net,NtiData);

% Denormalize
lsData = denormalize(NlsData,rawEMin,rawESpan);
leData = denormalize(NleData,rawEMin,rawESpan);
vsData = denormalize(NvsData,rawEMin,rawESpan);
veData = denormalize(NveData,rawEMin,rawESpan);
tsData = denormalize(NtsData,rawEMin,rawESpan);
teData = denormalize(NteData,rawEMin,rawESpan);

performance = mse(veData-vsData)
mseBest

% Figures
figure
axDim = [0 45];
plot(leData(2,:),lsData(2,:),'xb',veData(2,:),vsData(2,:),'xr',teData(2,:),ts
Data(2,:),'xg',axDim,axDim, 'k-');
axis([axDim axDim]);
axis square;
title('Ethylen');

figure
axDim = [0 25];
plot(leData(1,:),lsData(1,:),'xb',veData(1,:),vsData(1,:),'xr',teData(1,:),ts
Data(1,:),'xg',axDim,axDim, 'k-');
axis([axDim axDim]);
axis square;
title('Methan');

figure
axDim = [0 40];
plot(leData(3,:),lsData(3,:),'xb',veData(3,:),vsData(3,:),'xr',teData(3,:),ts
Data(3,:),'xg',axDim,axDim, 'k-');
axis([axDim axDim]);
axis square;
title('Propylen');

figure
axDim = [80 100];
%plot(leData(4,:),lsData(4,:),'xb',veData(4,:),vsData(4,:),'xr',teData(4,:),t
sData(4,:),'xg',axDim,axDim, 'k-');
axis([axDim axDim]);
axis square;
title('conversion');
```

denormalize function

```
function f = denormalize(x,offset,factor);
xrow = size(factor,1) - size(x,1) + 1;
f = x .* repmat(factor(xrow:end,:),1,size(x,2)) +
repmat(offset(xrow:end,:),1,size(x,2));
```

Annex C

Table C1: n-heptane

Temperature (ºC)	700	815
Flow (ml.min-1)	150	100
x (%)	7.0	87.6
Products	y (wt.%)	
Methane	0.4	7.2
Ethane	0.1	2.1
Ethylene	2.8	48.5
Propane	0.0	0.5
Propylene	1.2	15.5
Acethylene	0.0	0.6
2-Methylpropane	0.0	0.2
Propadiene	0.0	0.1
n-Butane	0.0	0.0
trans-2-butene	0.0	0.3
1-Butene	1. 0	5.1
2-Methyl-1-propene	0.0	0.1
cis-2-Butene	0.0	0.2
Propine	0.0	0.3
1,3-Butadiene	0.0	4.2
Cyclopentadiene	0.0	0.3
C5-C6 unidentified	1.7	1.8
Benzene	0.1	0.4
Toluene	0.0	0.1
Ethylbenzene	0.0	0.0
m+p-Xylene	0.0	0.0
Styrene	0.0	0.0
o-Xylene	0.0	0.0
Naphtalene	0.0	0.0
C7-C12 unidentified	0.0	0.0
oil	0.0	0.0

Table C2: n-octane

Temperature (ºC)	700	810
Flow ($ml.min^{-1}$)	200	100
x (%)	9.3	92.3
Products	Y (wt.%)	
Methane	0.6	8.6
Ethane	0.5	3.8
Ethylene	2.9	43.9
Propane	0.1	0.6
Propylene	1.4	17.2
Acethylene	0.0	0.4
2-Methylpropane	0.0	0.0
Propadiene	0.0	0.2
n-Butane	0.0	0.0
trans-2-butene	0.0	0.3
1-Butene	1.1	4.8
2-Methyl-1-propene	0.0	0.1
cis-2-Butene	0.0	0.3
Propine	0.0	0.3
1,3-Butadiene	0.1	5.2
Cyclopentadiene	0.0	0.7
C_5-C_6 unidentified	2.6	4.7
Benzene	0.0	0.0
Toluene	0.0	0.3
Ethylbenzene	0.0	0.0
m+p-Xylene	0.0	0.0
Styrene	0.0	0.1
o-Xylene	0.0	0.0
Naphtalene	0.0	0.0
C_7-C_{12} unidentified	0.2	0.8
oil	0.1	0.2

Table C3: n-dodecane

Temperature (ºC)	650	700	750	810
Flow ($ml.min^{-1}$)	100	200	400	100
x (%)	10.6	13.4	11.3	96.7
Products		y (wt.%)		
Methane	0.4	0.6	0.5	7.9
Ethane	0.4	0.5	5.3	3.4
Ethylene	1.7	3.0	2.6	43.2
Propane	0.0	0.1	0.1	0.6
Propylene	0.8	1.4	1.1	18.7
Acethylene	0.0	0.0	0.0	0.5
2-Methylpropane	0.0	0.0	0.0	0.0
Propadiene	0.0	0.0	0.0	0.1
n-Butane	0.0	0.0	0.0	0.0
trans-2-butene	0.0	0.0	0.0	0.4
1-Butene	0.6	1.0	0.8	5.8
2-Methyl-1-propene	0.0	0.0	0.0	0.1
cis-2-Butene	0.0	0.0	0.0	0.3
Propine	0.0	0.0	0.0	0.3
1,3-Butadiene	0.0	0.1	0.1	6.8
Cyclopentadiene	0.0	0.0	0.0	0.0
C_5-C_6 unidentified	2.0	3.5	3.0	7.3
Benzene	0.0	0.0	0.0	0.0
Toluene	0.0	0.0	0.0	0.5
Ethylbenzene	0.0	0.0	0.0	0.1
m+p-Xylene	0.0	0.0	0.0	0.1
Styrene	0.0	0.0	0.0	0.2
o-Xylene	0.0	0.0	0.0	0.0
Naphtalene	0.0	0.0	0.0	0.0
C_7-C_{12} unidentified	2.4	3.5	3.0	0.8
oil	2.8	0.2	0.3	0.1

Table C4: n-hexadecane

Temperature (ºC)	700	810
Flow (ml.min^{-1})	300	100
x (%)	10.6	98.7
Products	y (wt.%)	
Methane	0.4	7.7
Ethane	0.3	3.8
Ethylene	1.7	41.8
Propane	0.0	0.6
Propylene	0.7	19.1
Acethylene	0.0	0.4
2-Methylpropane	0.0	0.0
Propadiene	0.0	0.1
n-Butane	0.0	0.0
trans-2-butene	0.0	0.5
1-Butene	0.5	5.7
2-Methyl-1-propene	0.0	0.1
cis-2-Butene	0.0	0.4
Propine	0.0	0.3
1,3-Butadiene	0.0	7.6
Cyclopentadiene	0.0	0.0
C_5-C_6 unidentified	2.0	8.8
Benzene	0.0	0.0
Toluene	0.0	0.8
Ethylbenzene	0.0	0.1
m+p-Xylene	0.0	0.1
Styrene	0.0	0.2
o-Xylene	0.0	0.0
Naphtalene	0.0	0.0
C_7-C_{12} unidentified	2.6	1.0
oil	2.6	0.0

Table C5: 2-methylbutane

Temperature (ºC)	700	815
Flow (ml.min^{-1})	75	100
x (%)	10.5	77.9
Products	y (wt.%)	
Methane	1.3	12.2
Ethane	0.3	2.0
Ethylene	1.2	16.3
Propane	0.1	0.4
Propylene	2.1	19.8
Acethylene	0.0	0.3
2-Methylpropane	0.0	0.7
Propadiene	0.0	0.0
n-Butane	0.0	0.0
trans-2-butene	1.1	2.3
1-Butene	0.3	2.6
2-Methyl-1-propene	2.6	10.0
cis-2-Butene	0.7	1.8
Propine	0.0	0.0
1,3-Butadiene	0.4	3.6
Cyclopentadiene	0.0	1.0
C_5-C_6 unidentified	0.6	3.2
Benzene	0.0	0.5
Toluene	0.0	0.3
Ethylbenzene	0.0	0.0
m+p-Xylene	0.0	0.1
Styrene	0.0	0.0
o-Xylene	0.0	0.0
Naphtalene	0.0	0.0
C_7-C_{12} unidentified	0.0	0.4
oil	0.0	0.0

Table C6: 2-Methylheptane

Temperature (ºC)	700	815
Flow (ml.min^{-1})	150	100
x (%)	12.2	94.0
Products	y (wt.%)	
Methane	0.6	9.1
Ethane	0.3	2.2
Ethylene	3.0	34.6
Propane	0.1	0.5
Propylene	2.8	22.4
Acethylene	0.0	0.5
2-Methylpropane	0.0	0.6
Propadiene	0.0	0.1
n-Butane	0.0	0.0
trans-2-butene	0.0	0.4
1-Butene	0.7	3.6
2-Methyl-1-propene	1.7	6.1
cis-2-Butene	0.0	0.4
Propine	0.0	0.6
1,3-Butadiene	0.1	5.4
Cyclopentadiene	0.0	1.2
C_5-C_6 unidentified	2.4	3.2
Benzene	0.1	1.1
Toluene	0.2	0.5
Ethylbenzene	0.0	0.1
m+p-Xylene	0.0	0.1
Styrene	0.0	0.1
o-Xylene	0.0	0.0
Naphtalene	0.0	0.0
C_7-C_{12} unidentified	0.4	1.0
oil	0.1	0.1

Table C7: 3-Methylhexane

Temperature (ºC)	700	815
Flow (ml.min^{-1})	150	100
x (%)	12.3	94.2
Products	y (wt.%)	
Methane	1.0	12.4
Ethane	0.3	3.5
Ethylene	2.4	30.5
Propane	0.1	0.7
Propylene	3.2	21.3
Acethylene	0.0	0.6
2-Methylpropane	0.0	0.5
Propadiene	0.0	0.1
n-Butane	0.0	0.0
trans-2-butene	0.5	1.2
1-Butene	0.3	3.4
2-Methyl-1-propene	0.1	2.5
cis-2-Butene	0.4	0.9
Propine	0.0	0.7
1,3-Butadiene	0.1	6.7
Cyclopentadiene	0.1	2.0
C_5-C_6 unidentified	3.7	4.4
Benzene	0.1	1.5
Toluene	0.0	0.7
Ethylbenzene	0.0	0.1
m+p-Xylene	0.0	0.1
Styrene	0.0	0.1
o-Xylene	0.0	0.0
Naphtalene	0.0	0.0
C_7-C_{12} unidentified	0.0	0.3
oil	0.0	0.0

Table C8: 3-Methylheptane

Temperature (ºC)	700	815
Flow (ml.min^{-1})	150	100
x (%)	11.7	94.5
Products	y (wt.%)	
Methane	0.8	10.2
Ethane	0.2	3.2
Ethylene	2.6	37.1
Propane	0.1	0.6
Propylene	2.0	19.4
Acethylene	0.0	0.7
2-Methylpropane	0.0	0.6
Propadiene	0.0	0.1
n-Butane	0.0	0.0
trans-2-butene	0.4	1.0
1-Butene	1.1	4.2
2-Methyl-1-propene	0.1	2.3
cis-2-Butene	0.3	0.8
Propine	0.0	0.7
1,3-Butadiene	0.1	6.5
Cyclopentadiene	0.1	1.7
C_5-C_6 unidentified	2.4	3.4
Benzene	0.4	1.0
Toluene	0.8	0.0
Ethylbenzene	0.0	0.1
m+p-Xylene	0.0	0.1
Styrene	0.0	0.1
o-Xylene	0.0	0.0
Naphtalene	0.0	0.0
C_7-C_{12} unidentified	1.3	0.6
oil	0.1	0.0

Table C9: 3-Ethylhexane

Temperature (ºC)	700	815
Flow (ml.min^{-1})	200	100
x (%)	9.1	98,0
Products	y (wt.%)	
Methane	0.5	11.4
Ethane	0.2	3.9
Ethylene	2.0	40.0
Propane	0.1	1.0
Propylene	0.8	12.7
Acethylene	0.0	1.1
2-Methylpropane	0.0	0.4
Propadiene	0.0	0.1
n-Butane	0.0	0.0
trans-2-butene	0.0	0.5
1-Butene	1.5	5.3
2-Methyl-1-propene	0.0	0.7
cis-2-Butene	0.0	0.4
Propine	0.0	0.7
1,3-Butadiene	0.1	10.5
Cyclopentadiene	0.0	2.0
C_5-C_6 unidentified	3.4	4.1
Benzene	0.3	1.6
Toluene	0.0	0.5
Ethylbenzene	0.0	0.1
m+p-Xylene	0.0	0.1
Styrene	0.0	0.1
o-Xylene	0.0	0.1
Naphtalene	0.0	0.0
C_7-C_{12} unidentified	0.1	0.5
oil	0.0	0.0

Table C10: 2,2-Dimethylpentane

Temperature (ºC)	700	815
Flow (ml.min^{-1})	200	100
x (%)	8.2	95.5
Products	y (wt.%)	
Methane	0.5	13.7
Ethane	0.2	2.3
Ethylene	0.8	20.1
Propane	0.0	0.4
Propylene	1.4	11.4
Acethylene	0.0	0.4
2-Methylpropane	0.0	1.4
Propadiene	0.0	0.0
n-Butane	0.0	0.0
trans-2-butene	0.0	0.2
1-Butene	0.0	1.3
2-Methyl-1-propene	3.2	25.3
cis-2-Butene	0.0	0.2
Propine	0.0	1.3
1,3-Butadiene	0.0	1.8
Cyclopentadiene	0.5	4.2
C_5-C_6 unidentified	1.7	6.0
Benzene	0.0	2.1
Toluene	0.0	1.8
Ethylbenzene	0.0	0.1
m+p-Xylene	0.0	0.3
Styrene	0.0	0.1
o-Xylene	0.0	0.1
Naphtalene	0.0	0.0
C_7-C_{12} unidentified	0.0	0.7
oil	0.0	0.2

Table C11: 2,3-Dymethylpentane

Temperature (ºC)	700	815
Flow (ml.min^{-1})	200	100
x (%)	12.3	98.6
Products	y (wt.%)	
Methane	0.8	16.1
Ethane	0.3	2.8
Ethylene	1.0	17.6
Propane	0.1	0.7
Propylene	3.4	26.9
Acethylene	0.0	0.6
2-Methylpropane	0.0	0.5
Propadiene	0.0	0.1
n-Butane	0.0	0.0
trans-2-butene	0.9	2.1
1-Butene	0.4	3.5
2-Methyl-1-propene	0.1	2.1
cis-2-Butene	0.6	1.7
Propine	0.0	1.0
1,3-Butadiene	0.1	7.0
Cyclopentadiene	0.2	5.1
C_5-C_6 unidentified	4.4	5.1
Benzene	0.0	2.5
Toluene	0.0	1.5
Ethylbenzene	0.0	0.1
m+p-Xylene	0.0	0.2
Styrene	0.0	0.2
o-Xylene	0.0	0.1
Naphtalene	0.0	0.0
C_7-C_{12} unidentified	0.0	0.7
oil	0.0	0.2

Table C12: 2,4-Dimethylpentane

Temperature (ºC)	700	815
Flow (ml.min^{-1})	200	100
x (%)	10.1	92.9
Products	y (wt.%)	
Methane	0.5	11.8
Ethane	0.1	1.1
Ethylene	0.2	9.9
Propane	0.0	0.5
Propylene	4.1	36.9
Acethylene	0.0	0.4
2-Methylpropane	0.1	1.1
Propadiene	0.0	0.0
n-Butane	0.0	0.0
trans-2-butene	0.0	0.4
1-Butene	0.1	3.5
2-Methyl-1-propene	3.3	13.5
cis-2-Butene	0.0	0.3
Propine	0.0	0.8
1,3-Butadiene	0.0	3.7
Cyclopentadiene	0.7	1.7
C_5-C_6 unidentified	1.2	4.1
Benzene	0.0	1.5
Toluene	0.0	0.9
Ethylbenzene	0.0	0.1
m+p-Xylene	0.0	0.1
Styrene	0.0	0.1
o-Xylene	0.0	0.1
Naphtalene	0.0	0.0
C_7-C_{12} unidentified	0.0	0.4
oil	0.0	0.0

Table C13: 3,3-Dimethylpentane

Temperature (ºC)	700	815
Flow (ml.min^{-1})	200	100
x (%)	10.5	98.3
Products	y (wt.%)	
Methane	0.7	14.8
Ethane	0.3	4.3
Ethylene	2.4	24.2
Propane	0.1	0.8
Propylene	0.1	5.7
Acethylene	0.0	0.4
2-Methylpropane	0.0	1.4
Propadiene	0.0	0.1
n-Butane	0.0	0.0
trans-2-butene	0.0	0.3
1-Butene	0.0	0.8
2-Methyl-1-propene	2.4	20.6
cis-2-Butene	0.0	0.3
Propine	0.0	1.5
1,3-Butadiene	0.0	2.1
Cyclopentadiene	0.2	6.1
C_5-C_6 unidentified	4.3	8.0
Benzene	0.0	2.3
Toluene	0.0	2.1
Ethylbenzene	0.0	0.2
m+p-Xylene	0.0	0.5
Styrene	0.0	0.2
o-Xylene	0.0	0.2
Naphtalene	0.0	0.1
C_7-C_{12} unidentified	0.0	1.2
oil	0.0	0.3

Table C14: 2,2,3-trimethylbutane

Temperature (ºC)	700	815
Flow (ml.min^{-1})	250	100
x (%)	17.2	98.1
Products	y (wt.%)	
Methane	0.8	12.7
Ethane	0.4	1.6
Ethylene	0.3	11.2
Propane	0.0	0.5
Propylene	4.2	22.6
Acethylene	0.0	0.4
2-Methylpropane	0.1	1.9
Propadiene	0.0	0.0
n-Butane	0.0	0.0
trans-2-butene	0.0	0.2
1-Butene	0.1	1.8
2-Methyl-1-propene	5.5	24.3
cis-2-Butene	0.0	0.4
Propine	0.0	1.4
1,3-Butadiene	0.0	2.1
Cyclopentadiene	0.1	4.2
C_5-C_6 unidentified	5.7	6.6
Benzene	0.0	2.3
Toluene	0.0	1.9
Ethylbenzene	0.0	0.1
m+p-Xylene	0.0	0.4
Styrene	0.0	0.1
o-Xylene	0.0	0.2
Naphtalene	0.0	0.0
C_7-C_{12} unidentified	0.0	0.8
oil	0.0	0.2

Table C15: trans-2-octene

Temperature (ºC)	620	620	620	620	810
Flow ($ml.min^{-1}$)	50	100	200	300	100
x (%)	22.6	17.0	10.4	6.9	98.2
Products			y (wt.%)		
Methane	0.5	0.2	0.1	0.0	7.7
Ethane	0.3	0.1	0.0	0.0	2.7
Ethylene	3.5	1.7	0.7	0.3	48.6
Propane	0.0	0.0	0.0	0.0	0.8
Propylene	1.0	0.4	0.2	0.1	10.5
Acethylene	0.0	0.0	0.0	0.0	0.7
2-Methylpropane	0.0	0.0	0.0	0.0	0.2
Propadiene	0.0	0.0	0.0	0.0	0.1
n-Butane	0.0	0.0	0.0	0.0	0.0
trans-2-butene	0.1	0.0	0.0	0.0	0.5
1-Butene	1.4	0.6	0.3	0.1	2.1
2-Methyl-1-propene	0.1	0.1	0.1	0.1	0.4
cis-2-Butene	0.1	0.0	0.0	0.0	0.4
Propine	0.0	0.0	0.0	0.0	0.0
1,3-Butadiene	1.5	0.8	0.3	0.1	16.0
Cyclopentadiene	0.0	0.0	0.0	0.0	0.0
C_5-C_6 unidentified	3.6	1.6	0.9	0.6	3.8
Benzene	0.0	0.0	0.0	0.0	3.7
Toluene	0.0	0.0	0.0	0.0	0.8
Ethylbenzene	0.0	0.0	0.0	0.0	0.1
m+p-Xylene	0.0	0.0	0.0	0.0	0.0
Styrene	0.0	0.0	0.0	0.0	0.2
o-Xylene	0.0	0.0	0.0	0.0	0.0
Naphtalene	0.0	0.0	0.0	0.0	0.1
C_7-C_{12} unidentified	1.2	0.5	0.4	0.2	0.3
oil	0.1	0.1	0.5	0.7	0.2

Table C16: trans-3-octene

Temperature (ºC)	620	620	620	620	810
Flow ($ml.min^{-1}$)	50	100	200	300	100
x (%)	28.1	16.6	9.0	6.7	99.0
Products			y (wt.%)		
Methane	1.3	0.6	0.1	0.1	13.8
Ethane	0.6	0.3	0.0	0.0	6.0
Ethylene	3.6	1.8	0.5	0.3	36.3
Propane	0.1	0.1	0.0	0.0	1.0
Propylene	1.4	0.7	0.2	0.1	8.0
Acethylene	0.0	0.0	0.0	0.0	0.7
2-Methylpropane	0.0	0.0	0.0	0.0	0.1
Propadiene	0.0	0.0	0.0	0.0	0.1
n-Butane	0.0	0.0	0.0	0.0	0.0
trans-2-butene	0.0	0.0	0.0	0.0	0.3
1-Butene	0.5	0.2	0.1	0.0	1.4
2-Methyl-1-propene	0.0	0.0	0.0	0.0	0.1
cis-2-Butene	0.0	0,0	0.0	0.0	0.2
Propine	0.0	0.0	0.0	0.0	0.0
1,3-Butadiene	1.7	0.8	0.2	0.1	17.6
Cyclopentadiene	0.0	0.0	0.0	0.0	0.0
C_5-C_6 unidentified	7.2	3.2	1.4	0.6	5.9
Benzene	0.0	0.0	0.0	0.0	5.8
Toluene	0.0	0.0	0.0	0.0	1.4
Ethylbenzene	0.0	0.0	0.0	0.0	0.1
m+p-Xylene	0.0	0.0	0.0	0.0	0.1
Styrene	0.0	0.0	0.0	0.0	0.3
o-Xylene	0.0	0.0	0.0	0.0	0.1
Naphtalene	0,0	0.0	0.0	0.0	0.2
C_7-C_{12} unidentified	2.8	1.1	0.2	0.1	0.6
oil	0.3	0.4	0.5	0.4	0.0

Table C17: trans-4-octene

Temperature (ºC)	620	620	620	620	620	810
Flow ($ml.min^{-1}$)	50	100	200	300	400	100
x (%)	29.3	19.4	9.8	5.7	4.8	99.5
Products			y (wt.%)			
Methane	1.0	0.4	0.1	0.1	0.0	8.7
Ethane	1.0	0.3	0.1	0.0	0.0	4.3
Ethylene	5.1	2.9	1.2	0.6	0.4	45.9
Propane	0.3	0.1	0.1	0.0	0.0	2.0
Propylene	0.7	0.3	0.1	0.1	0.0	7.9
Acethylene	0.0	0.0	0.0	0.0	0.0	0.6
2-Methylpropane	0.2	0.1	0.0	0.0	0.0	0.1
Propadiene	0.0	0.0	0.0	0.0	0.0	0.4
n-Butane	0.0	0.0	0.0	0.0	0.0	0.0
trans-2-butene	0.0	0.0	0.0	0.0	0.0	0.3
1-Butene	0.3	0.1	0.1	0.0	0.0	1.5
2-Methyl-1-propene	0.0	0.0	0.0	0.0	0.0	0.1
cis-2-Butene	0.0	0.0	0.0	0.0	0.0	0.3
Propine	0.0	0.0	0.0	0.0	0.0	0.0
1,3-Butadiene	1.9	0.9	0.4	0.2	0.1	15.1
Cyclopentadiene	0.0	0.0	0.0	0.0	0.0	0.0
C_5-C_6 unidentified	9.7	5.5	2.3	1.2	0.8	5.0
Benzene	0.0	0.0	0.0	0.0	0.0	5.5
Toluene	0.0	0.0	0.0	0.0	0.0	1.2
Ethylbenzene	0.0	0.0	0.0	0.0	0.0	0.1
m+p-Xylene	0.0	0.0	0.0	0.0	0.0	0.1
Styrene	0.0	0.0	0.0	0.0	0.0	0.3
o-Xylene	0.0	0.0	0.0	0.0	0.0	0.1
Naphtalene	0.0	0.0	0.0	0.0	0.0	0.2
C7-C12 unidentified	2.6	1.3	0.6	0.2	0.2	0.5
oil	0.1	0.0	0.8	0.4	0.8	0.0

Table C18: 1-octene

Temperature (ºC)	620	620	620	620	620	810
Flow (ml.min$^{-1)}$	50	100	150	200	400	100
x (%)	22.8	13.2	7.8	9.1	5.7	99.5
Products			y (wt.%)			
Methane	0.3	0.1	0.1	0.0	0.0	4.3
Ethane	0.2	0.1	0.0	0.0	0.0	1.1
Ethylene	2.9	1.3	0.8	0.5	0.2	47.9
Propane	0.0	0.0	0.0	0.0	0.0	0.3
Propylene	1.9	0.8	0.5	0.3	0.1	21.7
Acethylene	0.0	0.0	0.0	0.0	0.0	0.5
2-Methylpropane	0.0	0.0	0.0	0.0	0.0	0.4
Propadiene	0.0	0.0	0.0	0.0	0.0	0.0
n-Butane	0.0	0.0	0.0	0.0	0.0	0.0
trans-2-butene	0.0	0.0	0.0	0.0	0.0	0.5
1-Butene	0.9	0.4	0.3	0.2	0.0	7.9
2-Methyl-1-propene	0.0	0.0	0.0	0.0	0.0	0.1
cis-2-Butene	0.0	0.0	0.0	0.0	0.0	0.4
Propine	0.0	0.0	0.0	0.0	0.0	0.0
1,3-Butadiene	1.1	0.5	0.3	0.2	0.0	9.4
Cyclopentadiene	0.0	0.0	0.0	0.0	0.0	0.0
C_5-C_6 unidentified	2.7	1.1	0.9	0.5	0.1	2.6
Benzene	0.0	0.0	0.0	0.0	0.0	1.8
Toluene	0.0	0.0	0.0	0.0	0.0	0.4
Ethylbenzene	0.0	0.0	0.0	0.0	0.0	0.0
m+p-Xylene	0.0	0.0	0.0	0.0	0.0	0.0
Styrene	0.0	0.0	0.0	0.0	0.0	0.1
o-Xylene	0.0	0.0	0.0	0.0	0.0	0.0
Naphtalene	0.0	0.0	0.0	0.0	0.0	0.0
C_7-C_{12} unidentified	1.2	0.5	0.0	0.1	0.0	0.3
oil	0.2	0.1	0.1	0.4	0.7	0.1